BUREAU OF ENGINEERING RESEARCH

The University of New Mexico

Albuquerque, New Mexico

A THEORETICAL AND EXPERIMENTAL STUDY OF LOW VOLTAGE, HIGH CURRENT DC TO AC CONVERTERS WHICH USE EITHER MAGNETORESISTORS, SUPERCONDUCTORS, HALL EFFECT DEVICES, OR THIN-FILM DEVICES

FINAL REPORT

By

Richard Bechtel
W. W. Grannemann

EE-131

December, 1965

This work was performed for
National Aeronautics and Space
Administration, Grant NsG 279-62

TABLE OF CONTENTS

Chapter I

INTRODUCTION

This report presents a final summary of all work completed to date by this laboratory on National Aeronautics and Space Administration Grant NsG 279-62. The work done centered on a study of the applicability of magnetoresistors, superconductors, and thin-film field effect devices as controlled rectifiers, and multiterminal Hall effect generators for use in a low-voltage, high-current d.c. to a.c. converter (LV-HC converter), and the design and analysis of associated circuitry for such converters. Such study was originated and stimulated by the need to seek new methods for converting the output of unconventional power sources to a more useable form. Present methods usually employ transistors, which in many cases have unsatisfactory characteristics.

Unconventional power sources, such as thermoelectric generators, fuel cells, solar cells, and thermionic generators all normally have a low-voltage, high-current operational characteristic. Typically, these power sources operate in the range of a fraction of a volt to 1.5 volts. This voltage range can be increased by series-connecting the units, but this tends to lower the reliability and economy of operation acutely. An alternative is to use a fraction of a volt, high current source and switch the current into a step-up transformer. The a.c. output from the transformer

can then be rectified and filtered to provide the d.c. voltage-current balance desired for on-board electronic equipment.

Presently, transistors, tunnel diodes, and other common solid-state active devices that are capable of efficiently handling extremely high currents (currents in excess of 100 amperes) at fractions of a volt are a rarity. For example, if one considers a particular species of transistor (the most common switching device currently in use), a 100-ampere Pacific epitaxial planar transistor, he is faced with a saturation resistance on the order of 0.01 ohms, making it quite inefficient at less than two volts input and a source current of 100 amperes.

Several LV-HC converter circuits using transistors have been studied by Electro-Optical System, Inc., and it was found that the best circuit was the so-called Dreisbach converter.[1] This circuit uses thirty-two matched power transistors in parallel connection. If transformer and circuit losses are neglected this circuit has a theoretical efficiency of 43% at 0.5 volts and 100 amperes. The study done at The University of New Mexico has shown that this efficiency figure may well be improved on, even at much higher current levels, by employing controlled rectifier type devices, connected in a suitable circuit for stepping up the voltage efficiently.

The search and study of suitable controlled rectifiers and closely associated devices eventually reduced to magneto-resistors, superconductors, thin-film devices, and Hall effect

devices. In conjunction, a "best" circuit was arrived at and theoretically analyzed to complete the desired converter function. Also a conventional magnetic circuit was set up and theoretically analyzed as a necessary element of the functioning of the three magnetically controlled devices included in those above. Also, experiments were performed in all areas as extensively as possible. Finally, a new technique for obtaining a high-amplitude, square-pulse magnetic waveform was disclosed and discussed.

The theoretical and experimental study of magnetoresistance controlled rectifiers is summarized in Chapter II. This study revealed: (1) theoretical expressions for the magnetoresistance effect and those device configurations selected as the most important to the project; (2) indium antimonide to be the best room temperature material; (3) bismuth to be the best cryogenic temperature material; and (4) new methods for fabricating magnetoresistors from these materials. From this it was found that the Corbino disk and one irregularly shaped sample had essentially the same characteristics and were the best of all geometries tested. Using these best geometries a switching-ratio, K, of 51.2 at 20,000 gauss was obtained for InSb at room temperature, and for bismuth a K value of 145 at 20,000 gauss at 80° K, and a value of 510 at 9500 gauss at 4.2° K was obtained. In addition, the zero field resistances were found to be low, which is most encouraging--on the order of 70 micro ohms at 4.2° K, with Bi; 140 micro-ohms at 80° K with Bi; and 4100 micro-ohms at room temperature with InSb.

A summary of the theoretical and experimental study of superconducting rectifiers is presented in Chapter III. This study revealed: (1) theoretical expressions to indicate the most important facets of superconductivity applicable to the project, (2) a breakdown of suitable materials to accomplish the function intended, (3) methods for inducing the switching action, (4) the best superconductor forms, and (5) fabrication techniques. From this study it was concluded that either wire or thin-film devices could be used as a controlled rectifier, although the former would not be suitable for high frequency use because of inductance effects. With either form the switching action can either be accomplished by modulating, with in-line Helmholtz coils, a constant magnetic field source of magnitude just less than the critical field, or by wrapping the sample with an a.c. driven switching coil in the presence of the same type of constant field source.

The analytical work on the converter is summarized in Chapter IV. There the selection of the best electrical circuit is presented, along with an analysis and computer solution of same, showing expressions for the most important parameters. It is shown that the best circuit employs a bridge connection of alternately stimulated pairs of controlled rectifiers. For such a circuit the maximum theoretical efficiency is 100% with the added advantage that no direct current flows in the transformer under optimum conditions. Finally, a conventional magnetic circuit is presented and analyzed.

In Chapters V and VI two other devices are summarily discussed for possible use in LV-HC conversion. These are the thin-film transistor, and a Hall effect device which offers some possibility for usage but is not held to be very promising. In the case of the Hall device the analysis was quite extensive and therefore is given greater emphasis herein. Some experimentation was also carried out for this device, in a multiterminal configuration, and an efficiency of about 40% was measured under less than optimum conditions.

Chapter VII contains an introductory discussion on the feasibility of using switchable superconductors as magnetic shields to provide the type of waveform desirable for driving the magnetically controlled rectifier elements of a bridge converter. Such a discussion is mainly theoretical. However, some experimental evidence is presented which is most promising. In this experiment a bismuth magnetoresistor was used as the controlled rectifier, and a thin niobium sheet was used to envelope it as a magnetic shield. The data demonstrated that magnetic shielding was accomplished and that switching occurred at about the magnetic field level expected for niobium.

Finally, some concluding remarks are made in Chapter VIII concerning the future outlook for the LV-DC controlled rectifier converter. It is pointed out that this converter has good potential, particularly in view of the following: (1) there now exists a superconducting material with a critical temperature (18.3° K) nearly in the range of liquid hydrogen, a present on-board consumable in space vehicles;

(2) superconducting material development is advancing regularly, with no upper limit on critical temperature or critical magnetic field yet approached; (3) the magnetoresistor controlled rectifier can function under high current conditions to meet future needs; and (4) perfection of the superconducting magnetic shield scheme could boost the converter efficiency to very competitive levels.

Chapter II

THE MAGNETORESISTOR AS A CONTROLLED RECTIFIER

In the LV-HC converter research program the first device selected for study was the magnetoresistor, due to its basic simplicity, possible high current capability, and low impedance. The study ultimately became the most extensive, both theoretically and experimentally, of all devices considered, due to a succession of promising characteristics that became evident with time. The most important findings and developments on this subject are outlined and discussed below.

2.1 The Theory of Magnetoresistance

In setting up the theoretical expressions for the magnetoresistance effect in both bismuth and indium antimonide, one must take a different approach with each because of the differences in their electrical behavior. He begins with the phenomenological equations, branches therefrom to the classical approach, which applies to simple metals such as bismuth in special cases, and finally sets up the special formulations for InSb to correspond with its known behavior. Finally, one may also be interested in how, approximately, the magnetoresistance effect varies with temperature.

2.1.1 The Phenomenological Equation

If a current-carrying conductor (or semiconductor) is placed in a magnetic field $\overline{H}$, the Lorentz force on a charge carrier with charge q and effective mass m is:[2]

$$\overline{F} = \frac{d\overline{P}}{dt} = q\,\overline{E} + q/c(\overline{v} \times \overline{H}) \qquad (1)$$

where:

$\overline{P} = m\overline{v}$ = charge carrier momentum

$\overline{v}$ = charge carrier velocity

$\overline{E}$ = electric field

$\overline{H}$ = magnetic field

c = velocity of light

For a material in which the momentum of the charge carrier is governed by a finite mean free time between collisions τ, the equation (1) becomes:

$$\frac{d\overline{P}}{dt} = \frac{\overline{P}}{\tau} = q\,\overline{E} + q/c(\overline{v} \times \overline{H}) \qquad (2)$$

With an assumption that the charge carrier occupies an energy level near the top of the valence band, then $\overline{P} = m\overline{v}$ and:

$$\overline{v} = \frac{q\tau}{m}\,\overline{E} + \frac{q\tau}{mc}\,(\overline{v} \times \overline{H}) \qquad (3)$$

A density ρ of positive charge carriers moving with velocity $\overline{v}$ results in a current density:

$$\overline{J}_p = \rho q\overline{v} = \rho q(\frac{q\tau}{m})\,\overline{E} + \frac{1}{c}(\frac{q\tau}{m})(\overline{J}_p \times \overline{H}) \qquad (4)$$

which can be rewritten as:

$$\overline{J}_p = \sigma_p\overline{E} + \mu_p/c\,(\overline{J}_p \times \overline{H}) \qquad (5)$$

where:

$\sigma_p = q\rho\mu_p$ = conductivity of material

μ_p = charge carrier mobility = $\frac{q\tau}{m}$

The equation (5) is referred to as the phenomenological equation describing the galvanomagnetic properties of a

positive-carrier type conductor under the influence of magnetic and electric fields.

For materials in which electrons are the only charge carrier, the equation describing the relationship between current density, electric field and magnetic field becomes:

$$\bar{J}_n = \sigma_n \bar{E} - \mu_n/c \ (\bar{J}_n \times \bar{H}) \qquad (6)$$

where the various parameters are defined for electrons rather than holes, as in equation (5).

If both types of carriers are significant, the phenomenological equation becomes:

$$\bar{J} = \sigma\bar{E} + \frac{1}{c} (\mu_p \bar{J}_p - \mu_n \bar{J}_n) \times \bar{H} \qquad (7)$$

where

$$\sigma = \sigma_p + \sigma_n = |e|(\mu_p \rho + \mu_n \eta)$$

$$\bar{J} = \bar{J}_n + \bar{J}_p \ |$$

η = density of negative charge carriers

Since the only materials considered were n-type, only equation (6) is of interest herein.

2.1.2 The Classical Magnetoresistance Effect

The application of a magnetic field to a current carrying conductor usually alters the resistivity of the conductor. The more common effect of the magnetic field is to increase the resistivity of the conductor, although some cases of negative magnetoresistance have been observed. For normal magnetoresistance it has been shown that the variation of resistivity

due to a magnetic field obeys Kohler's rule:[3]

$$\frac{\rho(H) - \rho_o}{\rho_o} = F\left(\frac{H}{\rho_o}\right) \qquad (8)$$

where

ρ_o = zero field resistivity

$\rho(H)$ = resistivity with applied field H

and F is a function depending only on the physical properties and geometrical configuration of the conductor being observed.

Equation (6) can be modified to a more suitable form in the following manner:

$$\bar{J} = \sigma\bar{E} - \mu/c\ (\bar{J} \times \bar{H}) \qquad (6)$$

One should then substitute (6) into the right hand side of the equation for $\bar{J}$ and solve for $\bar{J}$.

$$\bar{J} = \sigma\bar{E} - \mu/c \left\{\left[\sigma\bar{E} - \mu/c(\bar{J} \times \bar{H})\right] \times \bar{H}\right\}$$

$$\bar{J} = \sigma\bar{E} - \mu\sigma/c\ (\bar{E} \times \bar{H}) + \mu^2/c^2 \left[(\bar{J} \times \bar{H}) \times \bar{H}\right]$$

$$\bar{J} = \sigma\bar{E} - \mu\sigma/c\ (\bar{E} \times \bar{H}) - (\mu^2H^2/c^2)\ \bar{J}$$

$$\bar{J}\ (1 + \mu^2H^2/c^2) = \sigma\bar{E} - \mu\sigma/c(\bar{E} \times \bar{H})$$

$$\bar{J} = \left[\sigma/(1 + \mu^2H^2/c^2\right] \bar{E} - \left[(\mu/c)\sigma/(1 + \mu^2H^2/c^2)\right] (\bar{E} \times \bar{H})$$

From this equation, it is seen that for transverse $\bar{E}$ and $\bar{H}$ fields applied to a conductor with normal conductivity σ, the resultant current density in the conductor consists of

component parallel to the applied field and a component normal to the applied field. These components of current density can be interpreted as resulting from the product of a magnetic field dependent conductivity with the applied electric field, and the second component consists of the product of the same magnetic field dependent conductivity with a magnetic dependent electric field normal to the applied electric field. With this interpretation, equation (9) becomes:

$$\bar{J} = \sigma_H \bar{E} - \sigma_H \bar{E}_H \qquad (10)$$

where:

J = net current density,

$\sigma_H = \sigma/(1 + \mu^2 H^2/c^2)$ = effective conductivity

$\bar{E}$ = applied electric field

$E_H = (\mu H/c)|e|$ = resultant electric field normal to $\bar{E}$

On the basis of this equation, the resistivity of the material would vary quadratically with the applied magnetic field H, as

$$\rho_H \approx \frac{1}{\sigma_H} = \frac{1}{\sigma}\left[\frac{1}{1 + \mu^2 H^2/c^2}\right] \qquad (11)$$

The derivation of the magnetoresistance effect by this classical method is appropriate only for simple metals and degenerate semiconductors in which the energy surfaces are spherical, and the relaxation time is independent of energy. The classical derivation always has as its result a quadratic dependence of the resistivity on the magnetic field H. There

are many intermetallic and semiconductor compounds which, experimentally, do not behave in this manner. In order to explain the galvanomagnetic phenomena peculiar to these materials, more elaborate methods of analysis must be employed.

2.1.3 The Magnetoresistance Effect in InSb

Rather than the classical quadratic dependence of magnetoresistance on magnetic field, the compound semiconductor InSb displays a change in resistivity which is proportional to the magnetic field. The explanation of this deviation from the classical results has been investigated theoretically by a number of authors for restricted ranges of temperature and magnetic field. In particular, it has been shown that in a strong magnetic field electron motion normal to the field becomes quantized such that the density of electron energy levels and the scattering matrices become functions of the magnetic field.[4] These results have been applied to the investigation of magnetoresistance in InSb.[5] Several different scattering models have been assumed by the various authors, but the net conclusion in each case is that for high purity n-type InSb, the magnetoresistance is a linear function of H for values of H above a few hundred gauss. In weak fields, it has been shown that the magnetoresistance varies from a H^2 dependence to a linear dependence as the field is increased from 0 to a few hundred gauss.[6]

In those applications where the magnetic field is above a few hundred gauss the magnetoresistance of InSb is essentially a linear function of H. That is, the resistivity

of InSb can be expressed as

$$\rho_H = \rho_o (1 + SH) \qquad (12)$$

where:

ρ_H = resistivity in magnetic field H

ρ_o = zero field resistivity

S = proportionality constant

In general, the proportionality constant S is primarily a function of the mobility and the temperature. It is independent of the geometry of the InSb sample. The net magnetoresistance of an InSb sample is a function of its geometry.

2.1.4 Variation of Magnetoresistance with Temperature

As the temperature of an InSb specimen is decreased from room temperature ($300^{\circ}K$), the resistivity, mobility, and Hall constant increase by varying amounts.[7] Since the magnetoresistance exhibited by the specimen depends upon all three of these parameters, it is apparent that the magnetoresistance is also dependent upon the temperature.

A comprehensive theory of the variation of magnetoresistance with temperature is not available at the present time; however, it has been found, experimentally, that the magnetoresistance of a specimen increases with decreasing temperature. The greatest increase in magnetoresistance occurs at low and moderate values of magnetic fields. For high fields of 20 kilogauss or more, the magnetoresistance may exhibit very little change with decreasing temperature.

2.2 Magnetoresistance Device Analysis

Numerous device geometries were tested for their magnetoresistance properties in order to select those best suited for converter application. The list was ultimately reduced to a few which were then more carefully analyzed theoretically and experimentally. The theoretical analysis of these geometries is outlined below.

2.2.1 The Rectangular Slab Magnetoresistor

The rectangular slab of InSb, shown in Figure 1, which has a zero field resistivity σ_o may be considered.

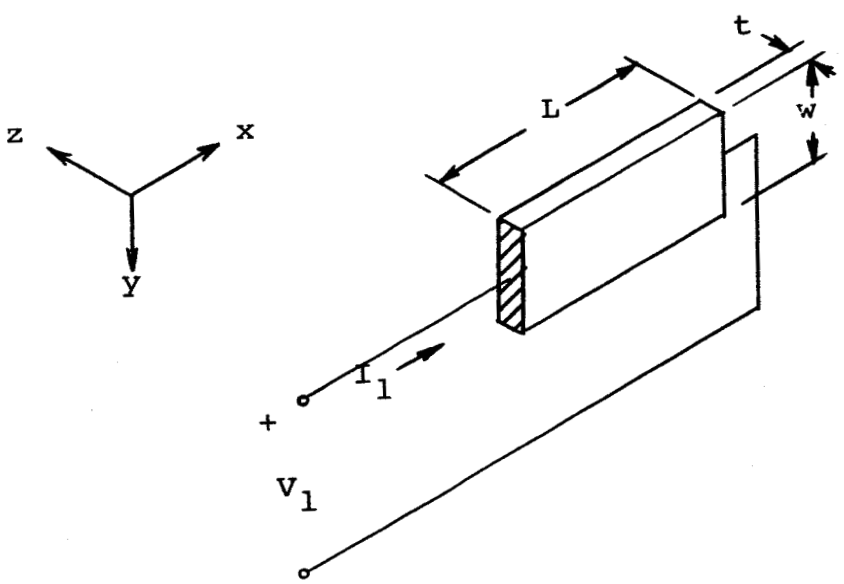

Figure 1. InSb Rectangular Slab

The zero field resistance of the slab is:

$$R_o = \rho_o \, L/wt \qquad (13)$$

It would appear that with a magnetic field H applied in the z direction, the resistance, R, of the slab would vary with H as

$$R = \rho_o \, L/wt \, (1 + SH) \qquad (14)$$

This is not the case, however, since a Hall field in the y direction results from the cross product of the current density and the magnetic field. The effect of this Hall field is to reduce the actual magnetoresistance of the slab below that predicted by equation (14) above, such that:

$$R = R_o(1 + K_1H) - K_2H \qquad (15)$$

where

$R_o = \rho_o \, L/wt$ = zero field resistance

K_1 = proportionality constant for bulk InSb

K_2 = proportionality constant due to geometry

The exact dependence of K_2 upon the geometry and the physical properties of InSb was not established since sufficient experimental data to determine the geometrical dependence of K_2 was not gathered. It has been found, however, that the value of K_2 can be sufficiently large to decrease the magnetoresistance of the rectangular slab to 1/3 that of the bulk material.

From the previous discussion, it is evident that in order to maximize the magnetoresistance of an InSb sample, the effect of the resultant Hall field on the magnetoresistance must be minimized. It has been found experimentally, for the rectangular slab, that the magnetoresistance could be increased by several percent if the lengthwise edges of the slab were electrically connected as shown in Figure 2.

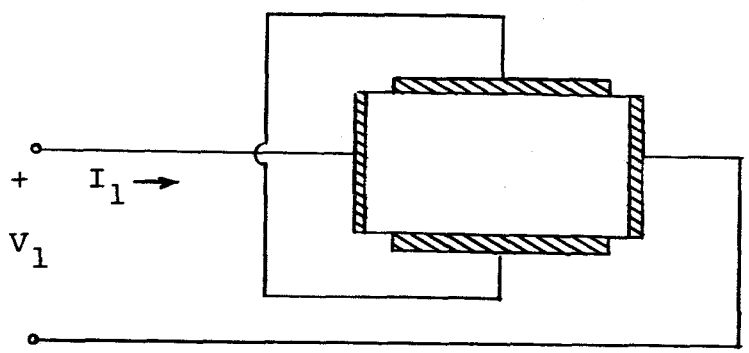

Figure 2. Modified Rectangular Slab

This modification of the slab results in a minimum Hall field being developed across the device, which in turn appears to reduce the value of K_2 in equation (15).

Later in this report when experimental evidence is presented for this device it will be shown that reduction of K_2, and thus reduction of the Hall field, does indeed increase the magnetoresistance.

2.2.2 The Symmetrical Four-Terminal Magnetoresistor

An interesting extension of the rectangular slab is shown in Figure 3. Here a square specimen with four symmetrical contacts is subjected to a transverse magnetic field H.

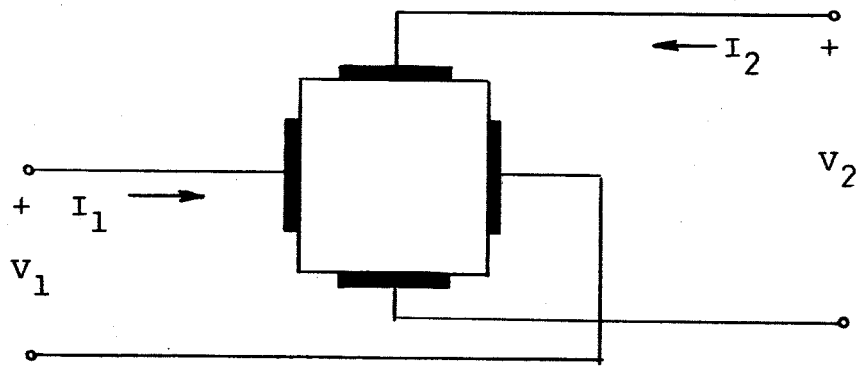

Figure 3. Duo-Magnetoresistor

The four-terminal open-circuit impedance equations for this configuration are:

$$V_1 = I_1 R_{11} + I_2 R_{12}$$

$$V_2 = I_1 R_{21} + I_2 R_{22} \qquad (16)$$

The R_{11} parameter is defined by:

$$R_{11} = V_1/I_1 \mid I_2 = 0$$

which is simply equation (15) for the rectangular slab with the appropriate values of K_1 and K_2 inserted. Because of the symmetry, the parameters R_{22} and R_{11} are equal, and have the value:

$$R_{11} = R_{22} = R_o(1 + SH) \qquad (17)$$

where $S = K_1 - K_2$

The parameter R_{12} is defined by:

$$R_{12} = \frac{V_1}{I_2} \mid I_1 = 0 \qquad (18)$$

which is simply the ratio of the Hall voltage to I_2, due to the cross product of I_2 and H. For the rectangular slab, the Hall voltage is:

$$V_1 = \pm \lambda H I_2 \qquad (19)$$

so that:

$$R_{12} = \pm \lambda H \qquad (20)$$

where λ is a constant of proportionality and the $\pm$ sign results from the direction dependence of the sign of the cross product $(\bar{I}_2 \times \bar{H})$. Again, because of the symmetry

$$R_{21} = -R_{21} = \pm \lambda H \tag{21}$$

where the negative value of R_{21} results from the direction dependence of the cross product $(\bar{I}_1 \times \bar{H})$.

With the values of the parameters determined above, the set of four-terminal equations become:

$$\begin{aligned} V_1 &= I_1 R_o (1 + SH) \pm \lambda H I_2 \\ V_2 &= I_2 R_o (1 + SH) \pm \lambda H I_1 \end{aligned} \tag{22}$$

If V_1 and V_2 represent identical low-impedance voltage sources, then:

$$V_1 = V_2 = V$$

and:

$$I_1 R_o (1 + SH) \pm \lambda H I_2 = I_2 R_o (1 + SH) \pm \lambda H I_1$$

which yields the ratio:

$$I_1/I_2 = \frac{R_o(1 + SH) \pm \lambda H}{R_o(1 + SH) \pm \lambda H} \tag{23}$$

This expression also represents the ratio R_2/R_1, where R_2 and R_1 are the input resistances:

$$R_2 = \frac{V_2}{I_2} = \frac{V}{I_2}$$

$$R_1 = \frac{V_1}{I_1} = \frac{V}{I_1}$$

It can be seen that when the magnetic field is in one direction, $R_2 > R_1$, and when the field is reversed, $R_1 > R_2$. Reversing the magnetic field has the effect of interchanging the roles of R_1 and R_2. When R_1 has a maximum value, R_2 is a minimum, and R_2 has a maximum value when R_1 is a minimum.

The characteristics of the input resistance of one terminal pair can be varied considerably by adjusting the current in the second terminal pair. For example, in equation (22), the voltage V_1 can be made zero for a field H by selecting I_2 to have the value:

$$I_2 = I_1 \frac{R_o(1 + SH)}{\lambda H} \tag{24}$$

Then:

$$V_1 = I_1 \left[R_o(1 + SH) \pm R_o(1 + SH)\right]$$

and the input resistance becomes

$$R_1 = V_1/I_1 = 2R_o(1 + SH) \tag{25}$$

for H in one direction, and:

$$R_1 = V_1/I_1 + 0 \tag{26}$$

for H in the opposite direction.

The experimental results agree quite well with the theoretical behavior predicted by equation (22).

2.2.3 The Corbino Disk Magnetoresistor

A geometrical configuration which has certain advantages over the rectangular slab is shown in Figure 4. This configuration is called a "Corbino disk" after O.M. Corbino

who in 1911 reported magnetoresistance measurements on several metals in which the samples were disks with inner and outer concentric ring contacts.[8]

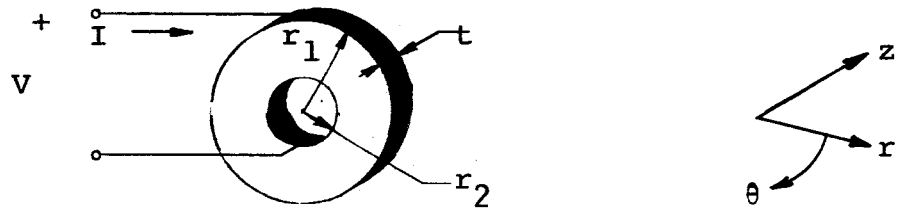

Note: r_1 = inner radius
r_2 = outer radius
t = thickness

Figure 4. Corbino Disk

In the absence of a magnetic field, the current flow is radial, and the zero field resistance of the disk is:

$$R_o = \frac{\rho_o}{2\pi t} \log_\epsilon \frac{r_2}{r_1}$$

where ρ_o is the zero-field resistivity.

With a magnetic field applied parallel to the axis of the disk, the current density will then have a component in the θ direction due to the radial component of current density. The only Hall field which can exist within the disk is parallel to its axis. This Hall field in the z direction results from the θ component of current density. Since the θ component of current density is proportional to the radial component, and the Hall field in the z direction is proportional to the θ component, the Hall field is proportional to the input current as in the case of the rectangular slab. In this situation, however, the proportionality constant relating the Hall field and the input current is small in comparison with that found in the rectangular slab. The resistance of the disk can be expressed as:

$$R = R_o(1 + K_1H) - K_2 F(H) \qquad (28)$$

where, again

R_o = zero field resistance

K_1 = proportionality constant of bulk InSb

K_2 = proportionality constant due to geometry

Here, F(H) is a function of the magnetic field. The equation (28) has the same form as (15) except that here, the subtraction factor is much less than that contained in (15). Also, the exact form F(H) takes is questionable. The theory of the disk presented above would indicate that F(H) is of the form:

$$F(H) = H + \lambda_1 H^2 \qquad (29)$$

The experimental data for various disks indicate no variation of resistance proportional to H^2 for fields above a few hundred gauss. Thus, it would appear that for fields up to 22 Kilogauss, the coefficient λ_1 is so small that the H^2 term can be neglected.*

2.2.4 Irregular-Shaped Magnetoresistors

In addition to the rectangular slab and the Corbino disk, various other geometrical configurations have been experimentally investigated. In general, these specimens have been the scraps which were left over from cutting rectangular slabs and disks from InSb ingots. Surprisingly enough, one of these rather odd-shaped pieces exhibited magnetoresistance characteristics on a par with the better modified rectangular slabs and Corbino disks. This unexpected, high magnetoresistance is attributed to the fact that the geometry and contact arrangement was such that the Hall effect was minimized.

2.3 Experiments with Magnetoresistors

Presented below are all the significant magnetoresistance experiment results and a summary of experimental and fabrication techniques that were developed. This will involve magnetoresistor samples of indium-antimonide and bismuth, the two materials selected for major study.

---

*This conclusion is valid only for high-purity, n-type, polycrystalline InSb. For example: Reference 7 lists results for single crystal InSb in which the magnetoresistance varies with H^2 for fields up to 4-6 Kilogauss, varies as H for fields of 6-15 Kilogauss, and then begins to approach a zero slope for fields in the vicinity of 20 Kilogauss.

2.3.1 Material Selection

The selection of bismuth as the low-temperature material was made by comparing the experimental results of several materials that are known to have a high mobility and low resistivity at cryogenic temperatures. The second best of these materials, tin, typically showed magneto-resistance about one-tenth that of comparable bismuth samples. Perhaps proper doping of tin could have improved its performance, but apparently it would never have surpassed bismuth. It was finally decided to concentrate solely on bismuth as the low-temperature material, since its performance was consistently good without resorting to elaborate procedures.

Doping effects in bismuth are another problem which was considered, and these results are discussed separately later on.

Indium-antimonide was selected as the room temperature material simply because of its very high mobility (65,000 cm^2/volt-sec) at this temperature.

2.3.2 Developed Specimen Preparation Techniques

2.3.2.1 Indium-Antimonide

It is well known that InSb is an extremely brittle material which is difficult to cut to a desired shape. Polycrystalline InSb, under strain or stress, has a tendency to break or shatter along the various grain boundaries. However, special cutting methods were developed by this laboratory for obtaining desired geometrical configurations from InSb ingots.

A motor-driven, self-sustaining, abrasive saw was designed and constructed for the purpose of cutting thin slices from a large ingot. The slices obtained from the ingot have a cross section of 1" x 3/4". The thickness of the specimen may be varied anywhere in the range 1/16" to 1". A maximum cross section of 2" x 2" can be cut by this saw. The cut is smooth with no evidence of fracturing.

The saw uses a mixture of water and fine mesh silicon carbide as an abrasive slurry. The specimen moves back and forth in this slurry with the cut made by a stationary diamond-impregnated bronze blade.

In addition to the motorized saw, an S. S. White Industrial 'Airbrasive' unit was used in conjunction with a turntable to cut circular disks from InSb slices. The saw can be used with a longitudinally moving platform to make straight line cuts in thin material.

The unit uses compressed air to supply a fine jet of abrasive material to the sample. This abrasive jet literally wears away the material to which it is applied. It is a rapid cutting tool, but can be used effectively only on slices of 3/16" or less in thickness.

The unit is ideally suited for cutting Corbino disks, even down to the cutting of the tiny center hole that receives the center contact.

2.3.2.2 Bismuth

Initially the bismuth samples were constructed from slices cut from a zone-refined bar of bismuth and moldings made by melting bismuth shot in carbon forms. Both the

bismuth shot and bar stock were of the same purity (99.9999%) and refinement. Tests showed that the molded samples eventually produced consistently higher magneto-resistance than the bar-stock samples. Thereafter the molding technique was used completely.

The molding was conducted under high vacuum using the apparatus shown in Figure 5. The molds were machined out of ultrahigh purity carbon for some samples and ordinary carbon for other sample runs.* The base block had the sample shape machined into it, and the top block was machined flat and served to press the molten metal into place. Of course, this apparatus is suitable only for flat samples, but there was no foreseeable need for any other type.

The entire apparatus was placed into a vacuum chamber and the heater current kept below that which would cause the metal pellets to melt until out-gassing was complete and a vacuum of 10^{-6} torr was obtained. After forming, the samples were allowed to cool sufficiently under vacuum to prevent oxidation.

---

*The effects of using these two different carbons will be discussed separately later on.

Molding Apparatus

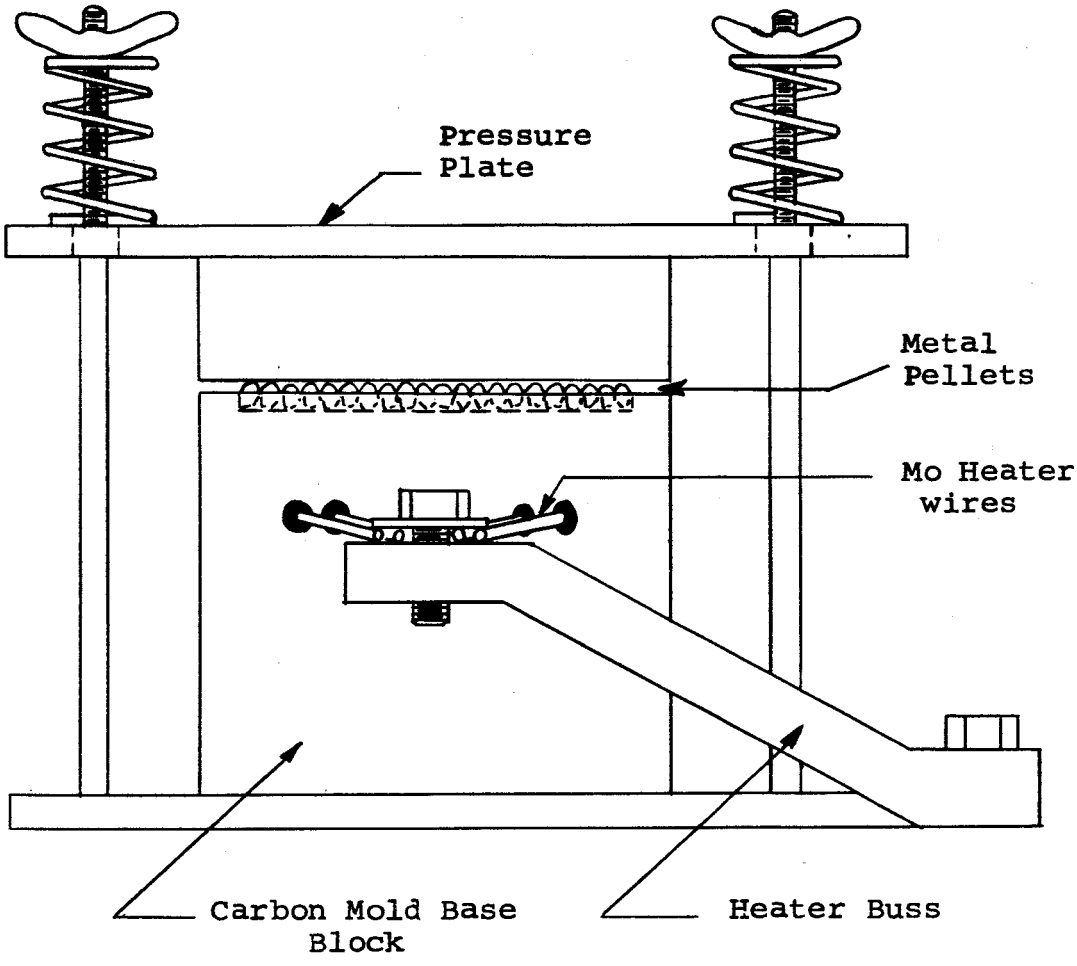

Figure 5

2.3.2.3 Application of Electrical Contacts

Prior to placing the electrical contacts on an InSb specimen, it was hand-lapped to the required shape and polished if desired. Then the specimen was etched in a solution with the following constituents:

2 parts by volume 70% HNO_3

1 part by volume 50% HF

1 part by volume 98% Glacial Acetic Acid

Diluted about 1/3 with distilled water or as desired.

The electrical contacts were made by using an ultrasonic soldering iron to apply pure indium to the contact area. Since pure indium is soft and malleable, it was found advisable to wet the contact area with a thin layer of indium and then to use an In-Pb-Sn solder for the bulk contact. This procedure resulted in a more stable low-resistance electrical contact.

Another method of contact application which proved useful for low temperature work was to vacuum deposit silver on the contact area. Then, a hard solder such as Pb-Sn or silver solder was used for the bulk contact.

A final method tried was to fuse indium into the InSb while the specimen was under high vacuum. This technique produced contacts of exceptional mechanical rigidity but with a higher resistance than desired at the junction. Efforts to decrease this resistance were not successful, but it is still possible that it could be done. If so, this would be a very desirable method.

Where application of electrical contacts to bismuth samples is concerned, no problems were encountered. Standard Pb-Sn solder results in good low resistance and mechanically rugged contacts.

2.3.3 Experimental Procedures

The schematic of the general circuit used in measuring the magnetoresistances of the various InSb and Bi specimens is shown in Figure 6.

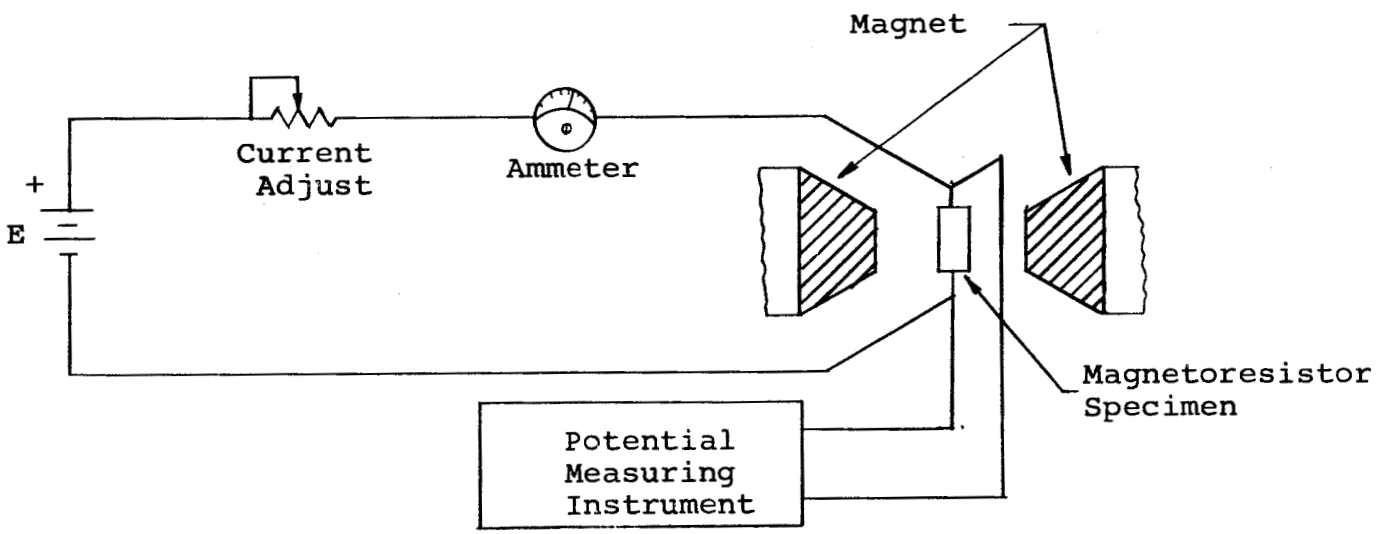

Figure 6. Test Circuit Schematic

The voltage source E was a 12-volt battery for low current measurements up to 15 amps. Three 6-volt batteries were connected in parallel to provide a source capable of supplying 200 amperes for five minutes into a 10-milliohm load.

The current was adjusted to the desired value by placing the proper resistance in series with the sample. The current was read on a calibrated ammeter to an accuracy of 1% or with a Hewlett Packard clip-on d.c. milliammeter.

The magnetic field was produced by a Varian electromagnet with 2-inch tapered pole pieces. This magnet can produce a field of 0-25 kilogauss, and has a means of reversing the direction of the field. The magnitude of the magnetic field was calibrated with an Empire Model 900 gaussmeter.

The potential measuring instrument was either a Leeds and Northrup K-2 potentiometer or a Millivac micro-voltammeter. The former instrument has high accuracy and resolution but is time consuming to operate. The latter instrument is fast and easy to use; however, its accuracy is on the order of $\pm$ 1%.

It should be pointed out that the leads for measuring the voltage drop across the specimen must be attached directly to the specimen's contacts; otherwise, a significant error is possible due to lead resistance.

All of the experimental data was obtained at either room temperature (300°K) or at cryogenic temperature (80°K and 4.2°K). The measurements at room temperatures were made with the specimen maintained at this temperature by forced-air cooling. The cryogenic measurements were made by placing the specimen in a special rectangular tail section dewar suspended between the poles of the magnet as shown in Figure 7.

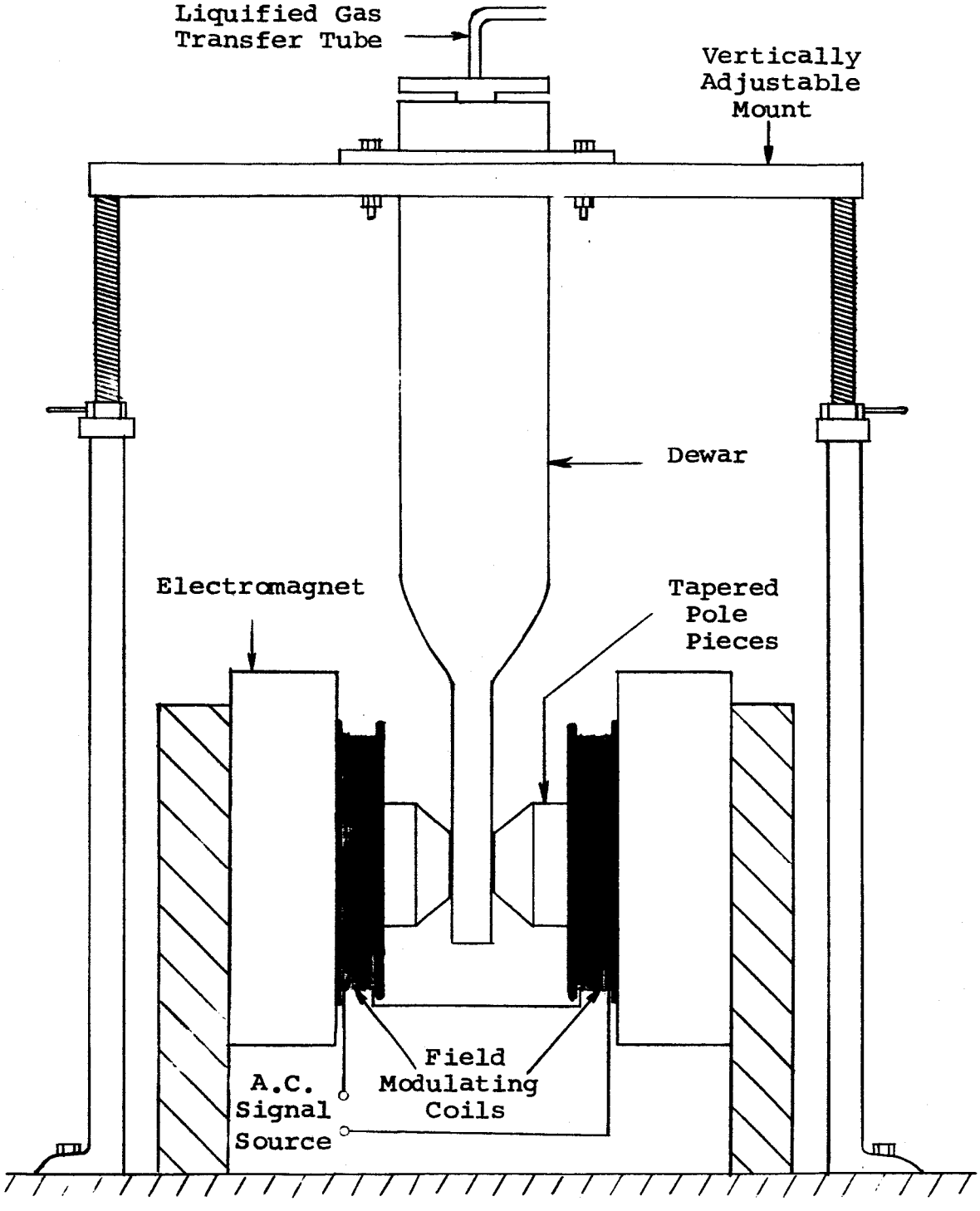
Liquified Gas
Transfer Tube
Vertically
Adjustable
Mount
Dewar
Electromagnet
Tapered
Pole
Pieces
A.C.
Signal
Source
Field
Modulating
Coils

Figure 7

2.3.4 Room Temperature Experimental Results (InSb)

In Figure 8 is shown the most important sample geometries that were tested at room temperature. Since several hundred magnetoresistor specimens were fabricated and tested during the project, only the best geometries will be presented here along with representative test results which are listed in Table I.

Data for Samples A and B illustrates the increase in magnetoresistance accomplished by shorting the Hall voltage (sample B) of an ordinary bar-type magnetoresistor (sample A). Data for sample C (a Corbino disk) shows the ultimate effect of Hall voltage elimination, a maximum magnetoresistance. The geometry of sample D is such as to reduce the Hall effect and thus result in a respectable magnetoresistance.

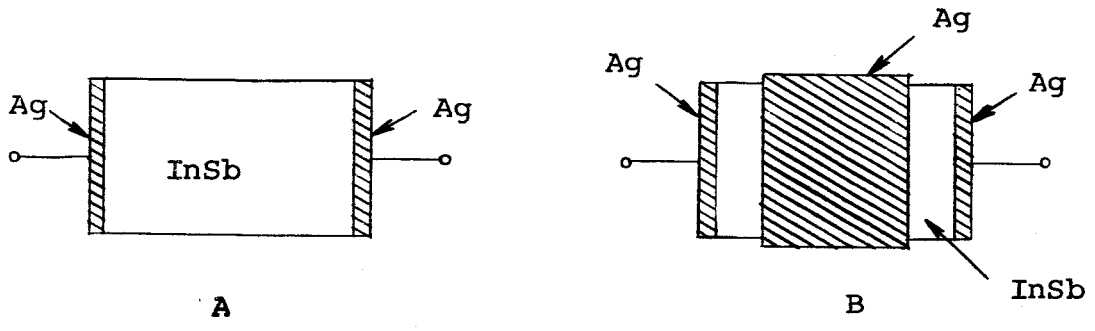

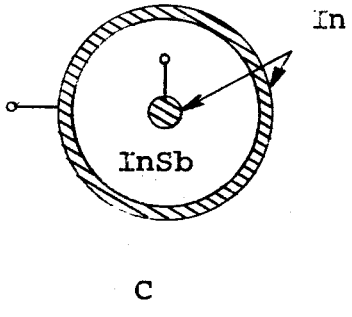

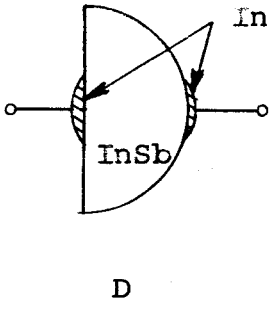

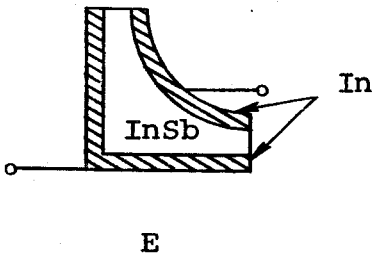

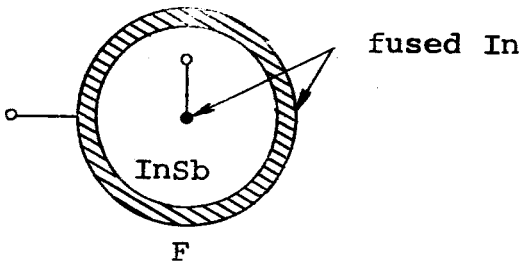

Figure 8

Indium Antimonide Sample Forms

TABLE I

Representative Test Data for the InSb Samples in Figure 8

Sample	Test Current (amps. d.c.)	Dimensions (cm) w = width t = thickness	Temp. (°K)	Field (Kilogauss)	$R/R_o = K$	R_o (ohms)
A*	1	1.1 (ℓ) x .05 (w) x .4 (t)	300	21.5	6.15	0.035
B*	1	1.1 (ℓ) x .05 (w) x .4 (t)	300	21.5	22.5	0.016
C**	1	1.8 (OD) x .48 (ID) x .32(t)	300	20.0	51.2	0.0041
D**	1	1.0 (radius)	300	20.0	28.0	0.007
E**	1	(from 1.8 cm square slice)	300	21.5	50.0	0.0035
F***	1	2.5 (OD) 0.1 (ID) 0.3 (t)	300	20.0	53.4	0.0147

*vacuum deposited silver contacts

**indium contacts, applied by ultrasonic soldering iron

***fused-indium contacts

Sample E represents a most useful discovery. It should be noticed that its total surface area and its magnetoresistance ratio $K = R/R_o$ is nearly that of sample C. This high value of K is, of course, attributable to the fact that the geometry greatly minimizes the Hall effect. Of additional interest is the fact that this sample's contact area is larger than that of sample C; therefore, sample E would seem preferable for larger current applications, if a small loss in magnetoresistance could be tolerated.

The data for sample F illustrates two characteristics of interest. The center contact diameter to outer contact diameter ratio is larger for this sample than for sample C, which resulted in an increased magnetoresistance, which is theoretically predictable. Second, the increased resistance resulting from using fused indium contacts is illustrated.

In Figures 9-11 are shown plots of K versus magnetic field for samples A and B, C and E, respectively. These figures clearly indicate the linear dependence that is expected for InSb, as was pointed out in Section 2.13.

2.3.5 Experimental Results at Cryogenic Temperatures (Bismuth)

Low temperature experiments with bismuth magnetoresistors were carried out at liquid nitrogen temperature ($80^{\circ}K$) for an initial test of characteristics, and then, when it was possible, at liquid helium temperature (4.2° K). Those samples of most interest are shown in Figure 12. Corbino disks, such as those shown as sample B, were subjected

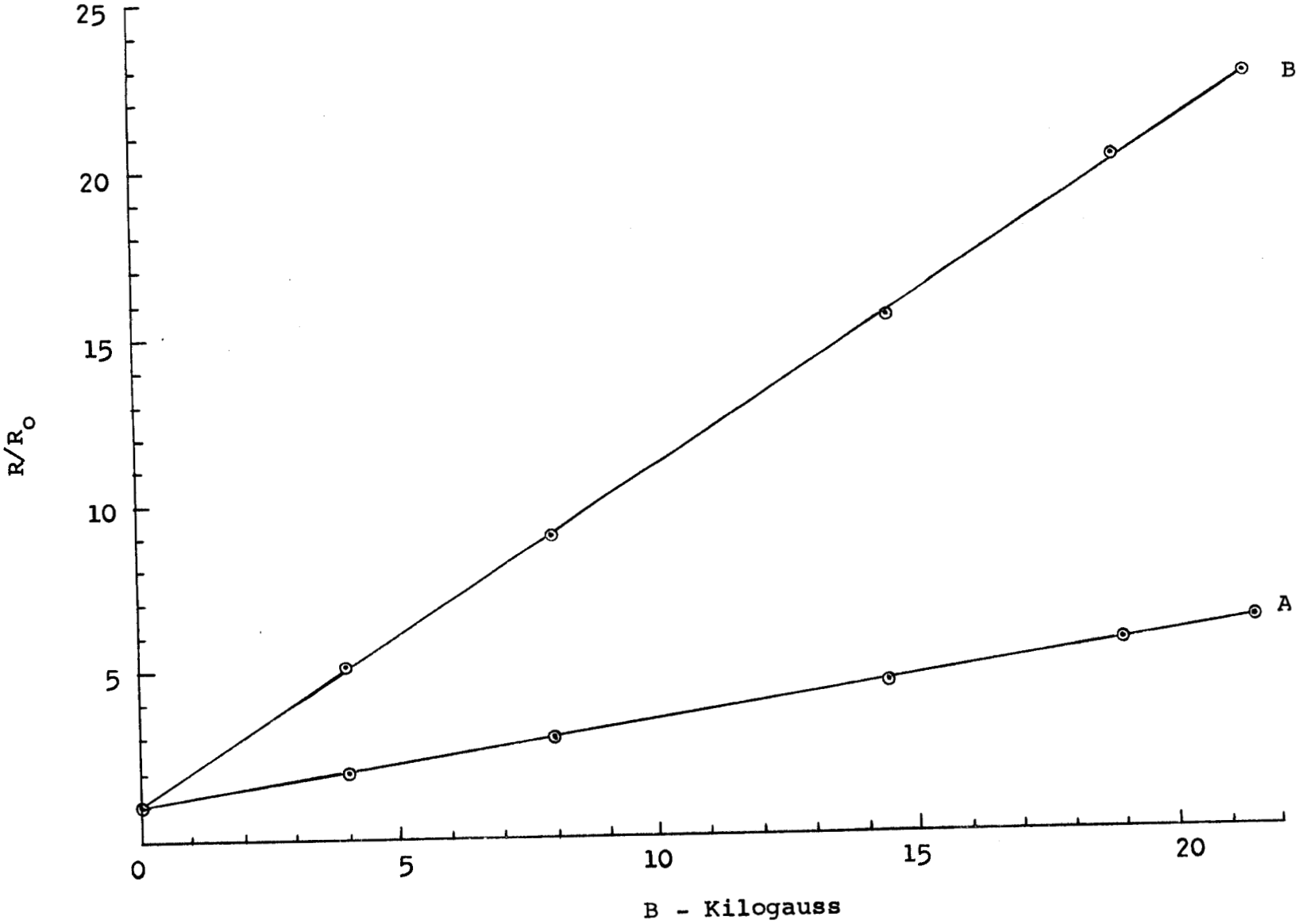

Figure 9

Rectangular Specimen:
A) regular bar-type
B) with Hall shorting contacts

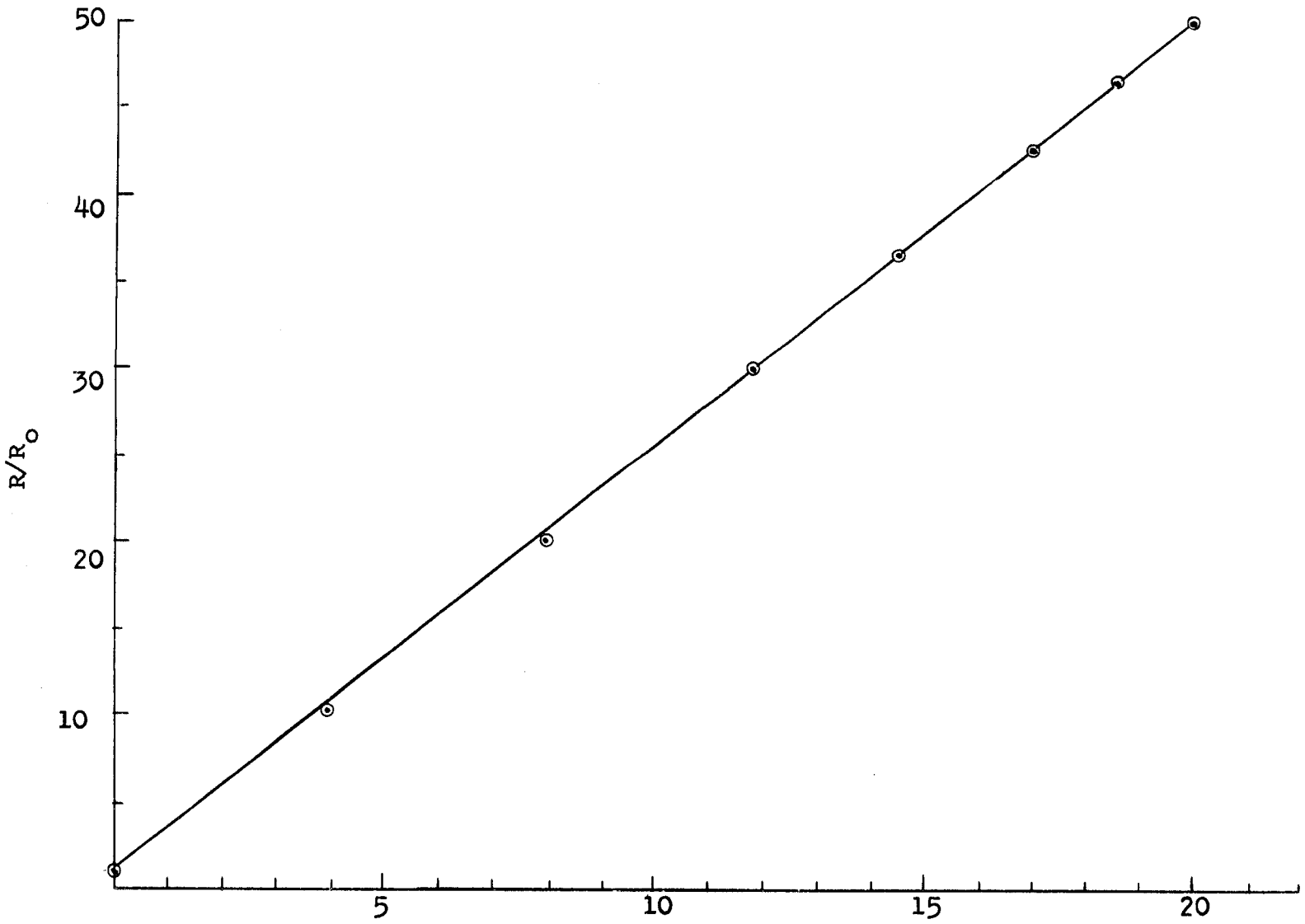

Figure 10

Corbino Disk, Sample C

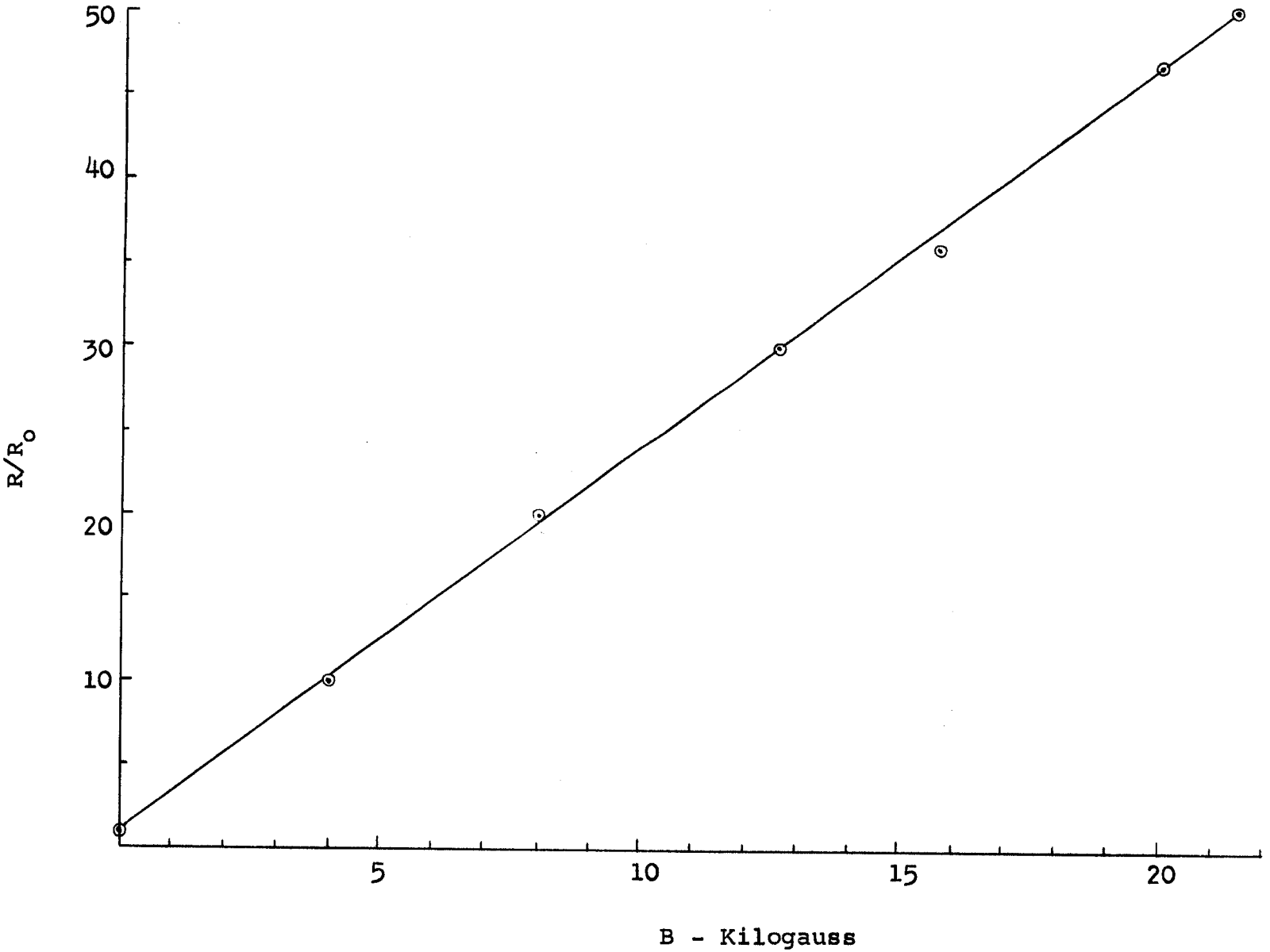

Figure 11

Irregular Geometry, Sample E

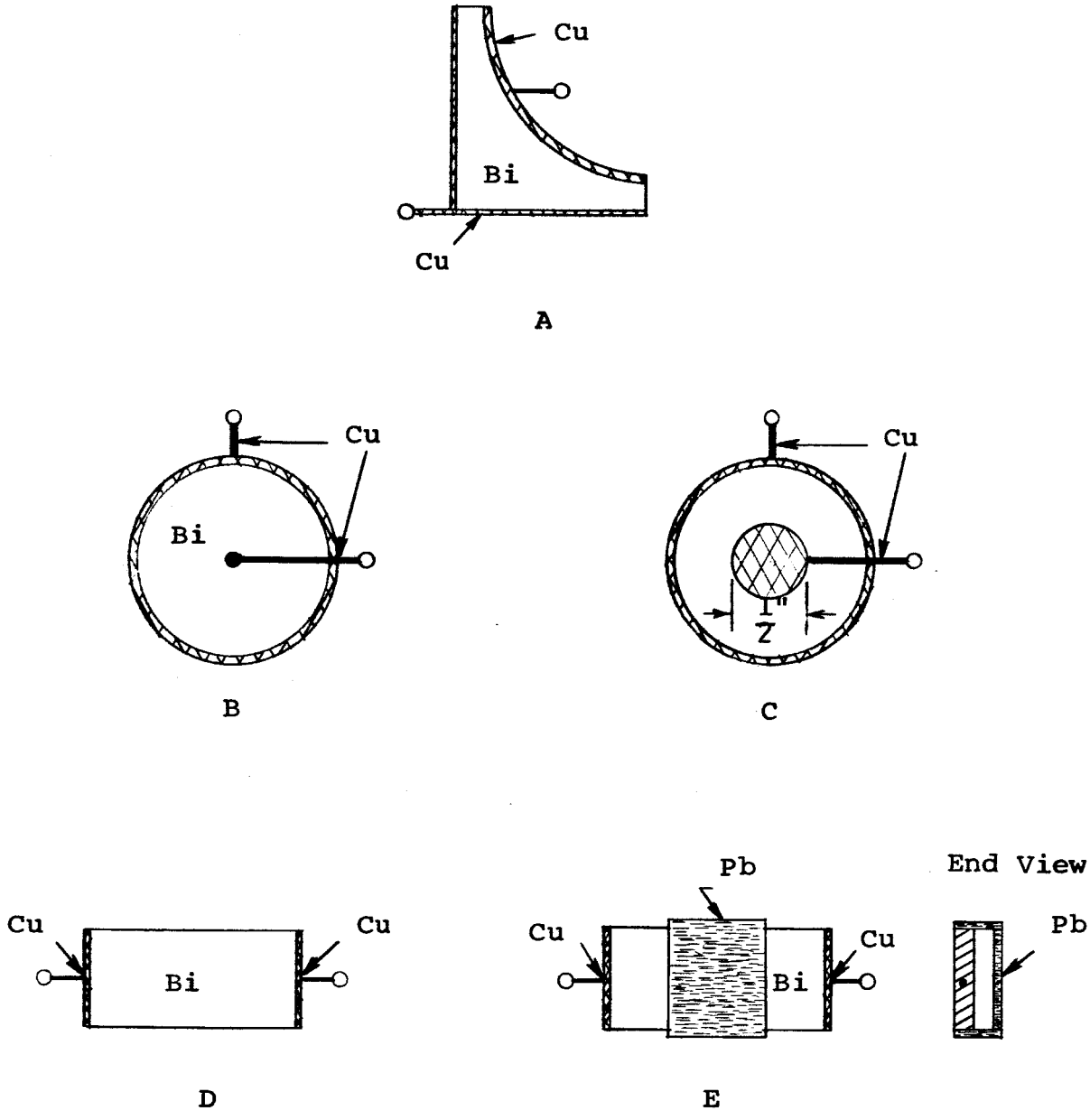

Figure 12

Bismuth Magnetoresistance Samples

to the most experimentation and provided the geometry used in a variety of other tests requiring a magnetoresistor. This was because of the disk's high K value, size for size, and its simplicity in being made by the molding technique.

2.3.5.1 Results at 80° K

Representative data for bismuth samples of the type shown in Figure 12 is listed in Table II. Upon examination of this data, one sees immediately that all the special features found for these sample geometries when InSb was used (discussed in Section 2.34) are again evident when bismuth is used. Therefore, these characteristics are not due to the material but rather the geometry which supports that which has been discussed previously.

Another statement that was made earlier was that bismuth should follow the classical, quadratic magnetoresistance dependence on magnetic field. This inclination is evident when one examines Figures 13-15, which show K versus magnetic field for samples A, B, and E, respectively.

2.3.5.2 Results at 4.2° K

Due to a seemingly endless variety of problems in obtaining from industry a liquid helium dewar without thermal leaks (leaks that prevent retention of the liquid), experimentation at 4.2° K was not near the extent planned for. However, the small amount of data that was obtained was quite encouraging. For example, a large diameter (4 cm) bismuth corbino disk magnetoresistor tested at 4.2° K was found to

TABLE II

Representative Test Data for Bismuth Samples in Figure 12

Sample	Test current (amps. d.c.)	Temperature (^{o}K)	Field kilogauss	$K = R/R_o$
A	10	80	14*	63.3
B	10	80	14*	71
B	10	80	20**	145
C	10	80	14*	6.7
D	40	80	14*	38
E	40	80	14*	54

* Limited to 14,000 gauss due to thickness of the tail section of the special dewar used for these samples.

** This sample was measured in a thin, plastic container that permitted brief runs with liquid nitrogen.

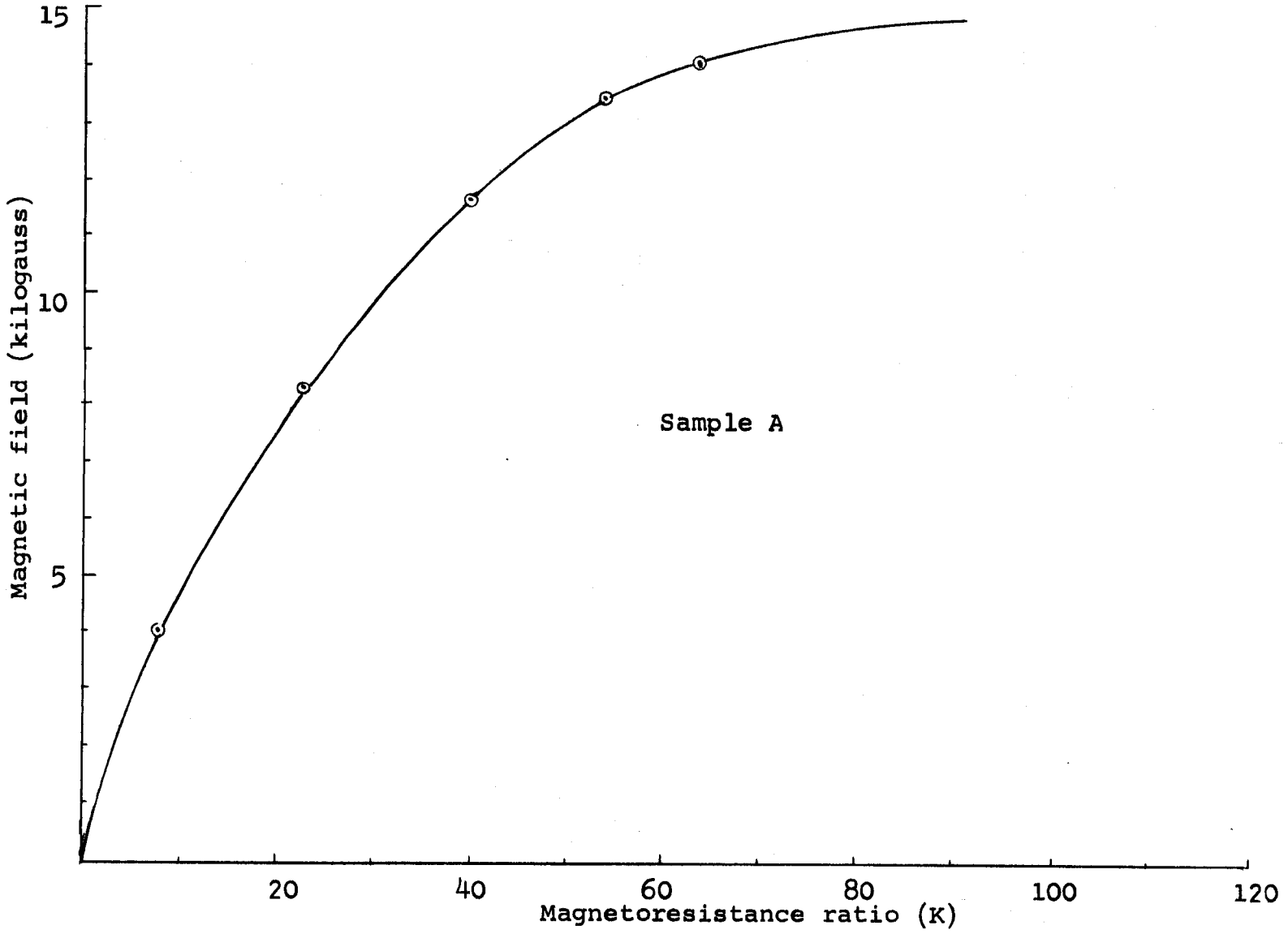
15
10
5
Magnetic field (kilogauss)
Sample A
20
40
60
80
100
120
Magnetoresistance ratio (K)

Figure 13

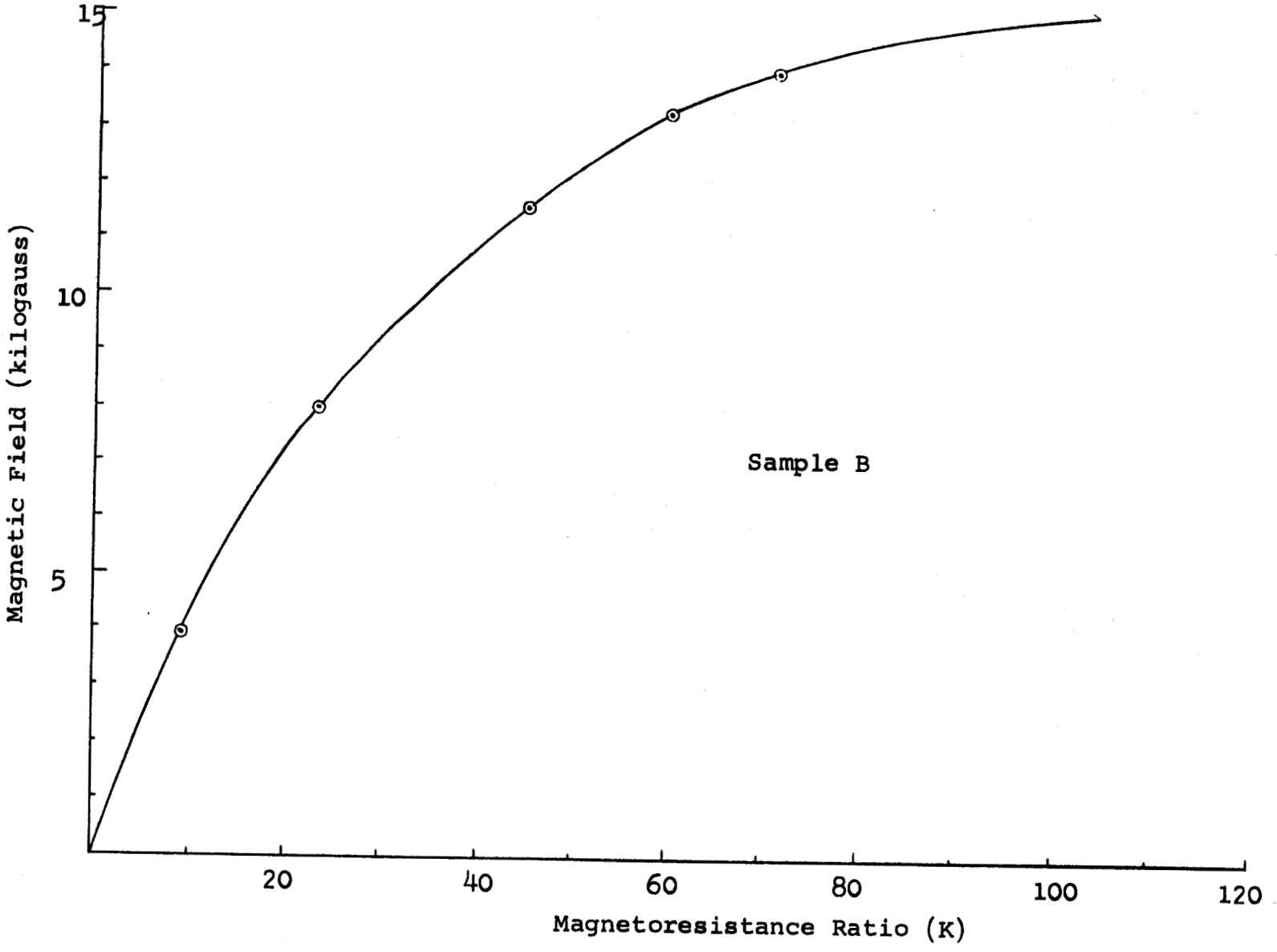
15
10
5
Magnetic Field (kilogauss)
Sample B
20
40
60
80
100
120
Magnetoresistance Ratio (K)

Figure 14

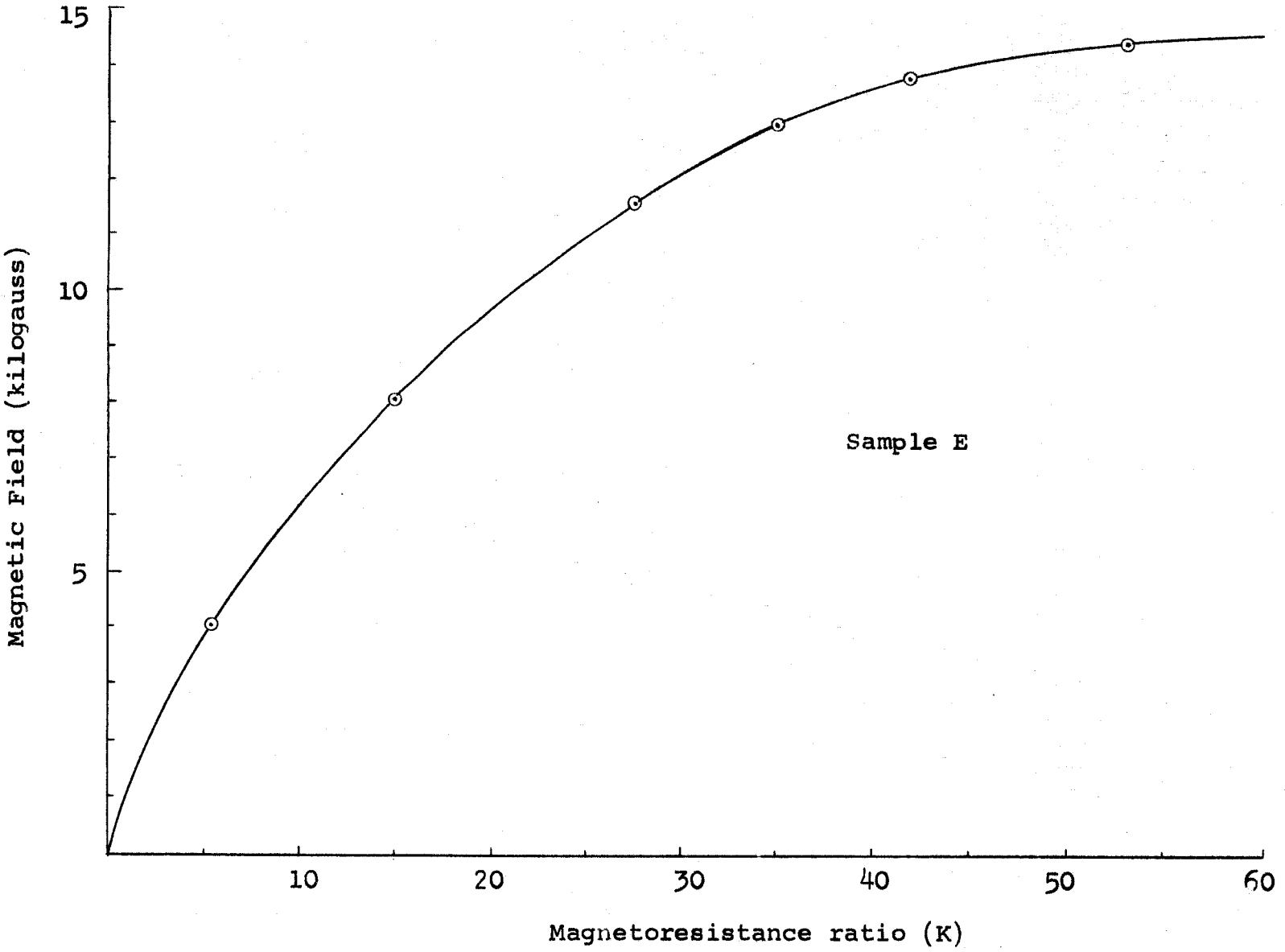
15
10
5
Magnetic Field (kilogauss)
Sample E
10
20
30
40
50
60
Magnetoresistance ratio (K)

Figure 15

have a K value of 1000 at 14 kilogauss. Of additional interest was the extremely low off-field resistance of this sample--125 micro-ohms.

Unfortunately, circumstances did not permit a test at 4.2° K involving sample E of Figure 12. The fact that the shunt was constructed using lead was very purposeful. Lead is a superconductor at 4.2° K, at fields less than its critical magnetic field; thus, one would have been able to observe the effects of a perfect Hall effect shunt on increasing the magnetoresistance of a bar sample. This would be of interest because a bar geometry is one also capable of high currents due to its large contact area, compared to that of a Corbino disk of comparable size.

Even though runs at 4.2° K were not able to be made, the results of the runs at 80° K indicate that the idea of a superconductive Hall effect shunt holds promise.

2.3.5.3 Experiments With Doping of Bismuth

Although the bismuth Corbino disks that were made without intentional doping had extremely good magnetoresistance compared to other published results, it was decided to try doping following the lead of Kleinman and Schawlow.[9] The tests showed that intentional doping to any measurable extent using tellurium only served to reduce the magnetoresistance of molded samples in every case. However, it had been noticed at one time previous to this that a higher magnetoresistance could be obtained, sample for sample, if the molding was done in a mold machined from a poor grade carbon

rather than one made from ultra-pure carbon. From this, if it was indeed repeatable, one could conclude that the proper doping level was nearly unmeasurable by conventional means, being the difference in impurity percentage existing in the two carbons. Several verification experiments were conducted along this line, and the results are discussed below.

The first step in the verification procedure was to machine dimensionally identical Corbino disk molds, one from standard, low-grade (LG), impure carbon, and another from zone-refined, ultra-high purity (HG) carbon. A double heater system was then constructed and installed in the bell jar of the vacuum system. This allowed simultaneous molding to be conducted to rule out differences in magnetoresistance characteristics that might occur due to different vacuum levels, melt-down times, hold times, and cool-down times. Several bismuth Corbino disk pairs, one LG sample, and one HG sample, for each run, were molded, then immediately measured for their characteristics in a special dewar at liquid nitrogen temperature. The results for a typical four-run set are presented in Table III. This data shows what consistently was found to be true for many run sets--samples molded in impure carbon had higher magnetoresistance (30% higher on the average) than did samples molded in ultra-pure carbon. This indicates that the proper doping level that maximizes the magnetoresistance of bismuth is really exceedingly low. This conclusion is also supported by consideration of data obtained from a deliberate-doping experiment that was conducted as follows.

The procedure for deliberate-doping was to use a fresh mold and to make the first disk using just bismuth. For the next run, in the same mold, one grain of tellurium powder was used as a doping agent.

TABLE III

DOPING EFFECTS

Representative Data on Bismuth Corbino Disks Molded Simultaneously in a Low-Grade (LG) and High-Grade (HG) Carbon Mold.

Sample*	Test current (amps. d.c.)	Temperature (^{o}K)	Field kilogauss	$K = R/R_o$	$R_o \times 10^6$
1 HG	1.8	80	9.5	33.3	175
1 LG	1.8	80	9.5	42.5	167
2 HG	1.8	80	9.5	26.0	140
2 LG	1.8	80	9.5	27.5	220
3 HG	1.8	80	9.5	31.0	195
3 LG	1.8	80	9.5	54.0	110
4 HG	1.8	80	9.5	36.0	110
4 LG	1.8	80	9.5	40.0	110

Mold Type	Average $K = R/R_o$	Average $R_o \times 10^6$
HG	31.5	155
LG	40.5	152

* Common numerical prefix indicates the simultaneity of runs, i.e., 1 LG and 1 HG were molded at the same time under identical conditions.

Then succeeding runs were made in the same mold with no doping agent added; the idea being that with the initial doping, some portion of the doping agent would be absorbed by the carbon to be returned to the molten material in succeeding runs.

Examination of the data compiled for the doping experiment revealed support of the aforementioned conclusion that the proper doping level is exceedingly small. Table IV contains a typical set of data for this experiment. It should be pointed out that the same trends were obtained regardless of the carbon material used. Of most dramatic interest, however, is the maximum level that was obtained for the high purity carbon mold run. This was sample 10 HG. It can be seen that this maximum exceeded the best obtained for the low-purity runs shown in Table III. Also characteristics of the best doped sample in the LG run, sample 13 LG, does not in any way mean that the optimum doping level was reached here. Of course, this same statement can be made about the HG run also.

Unfortunately, time did not permit further study of the doping problem to isolate best doping agents and determine optimum doping levels, but it is felt that what has been revealed is of significance.

2.4 Conclusion

It is believed that the theoretical and experimental study into the magnetoresistor, a device under consideration as a controlled rectifier, was revealing and valuable if not complete.

It was shown that the theoretical expectations were substantially verified by experiment. However, more experimental data is needed before the exact dependence, including time dependence, of the magnetoresistance upon the physical properties and geometries of the samples can be determined.

TABLE IV

Representative Test Data for Doping of Bismuth with Tellurium and Residual* (Mold-Absorbed Tellurium). An Experiment to Indicate Proper Doping Levels for Bismuth

Sample**	Doping Procedure	Test current (amps. d.c.)	Temperature (^{o}K)	Field kilogauss	$K=R/R_o$	$R_o \times 10^6$
10 LG	Bismuth + 1 grain Te powder	1.0	80	9.5	8.4	125
11 LG	Bismuth + residual from 10 LG	1.0	80	9.5	16.6	150
13 LG	Bismuth + residual from 10 LG, 11 LG	1.0	80	9.5	35.8	145
15 LG	Bismuth + residual from 10 LG, 11 LG, 12 LG, 13 LG	1.0	80	9.5	33.7	205
7 HG	Bismuth + 1 grain Te powder	1.0	80	9.5	9.4	250
8 HG	Bismuth + residual from 7 HG	1.0	80	9.5	11.6	370
10 HG	Bismuth + residual from 7 HG, 8 HG	1.0	80	9.5	47.5	145

* Residual: Any percentage of the Te dopant absorbed by the carbon molds from a previous run and thus left as a doping agent for the next run.

** All samples were nearly dimensionally identical. They were Corbino disks with a 1 1/4" diameter and a mean thickness of .085".

The study revealed materials that could be used with good results over a temperature span from room temperature to cryogenic temperature. Additionally, the techniques for handling these materials was successfully developed, complete to the fabrication of samples.

The high switching ratio (K) that was consistently obtained for Corbino disks and some other promising geometries that were discovered, using bismuth at low temperature or InSb at room temperature, would indicate that the magnetoresistor could well be an answer to the LV-HC converter requirements.

CHAPTER III
THE SUPERCONDUCTOR AS A CONTROLLED RECTIFIER

3.1 A Brief Account of the Theory of Superconductivity

In 1913 Kamerlingh-Onnes made the significant discovery that at each transition temperature there existed a critical magnetic field (H_c), at which the superconductivity was destroyed (see Figure 16). Therefore, if the surface of a superconductor is subjected to a magnetic field equal to its critical field, whether this field be generated by an external source or occurs due to internal current flow or a combination of these sources, a transition to the normal state is initiated.

However, since the time when Kamerlingh-Onnes first discovered the phenomenon of superconductivity, a complete theory for it has been sought, a microscopic theory from which there can be derived from first principles the regularities in the appearance of superconductivity as noted by Matthias.[10] The principle regularities are as follows:

1. Superconductivity has been found only for those metallic substances having between about 2 and 8 valence electrons.
2. Where transition metals are concerned, the variation in the critical temperature with the number of valence electrons shows sharp peaks for this number equaling 3, 5, and 7.
3. For a given number of valence electrons, certain crystal structures appear more favorably than others. In addition, the critical temperature increases with a high power of the atomic volume and inversely with the atomic mass.

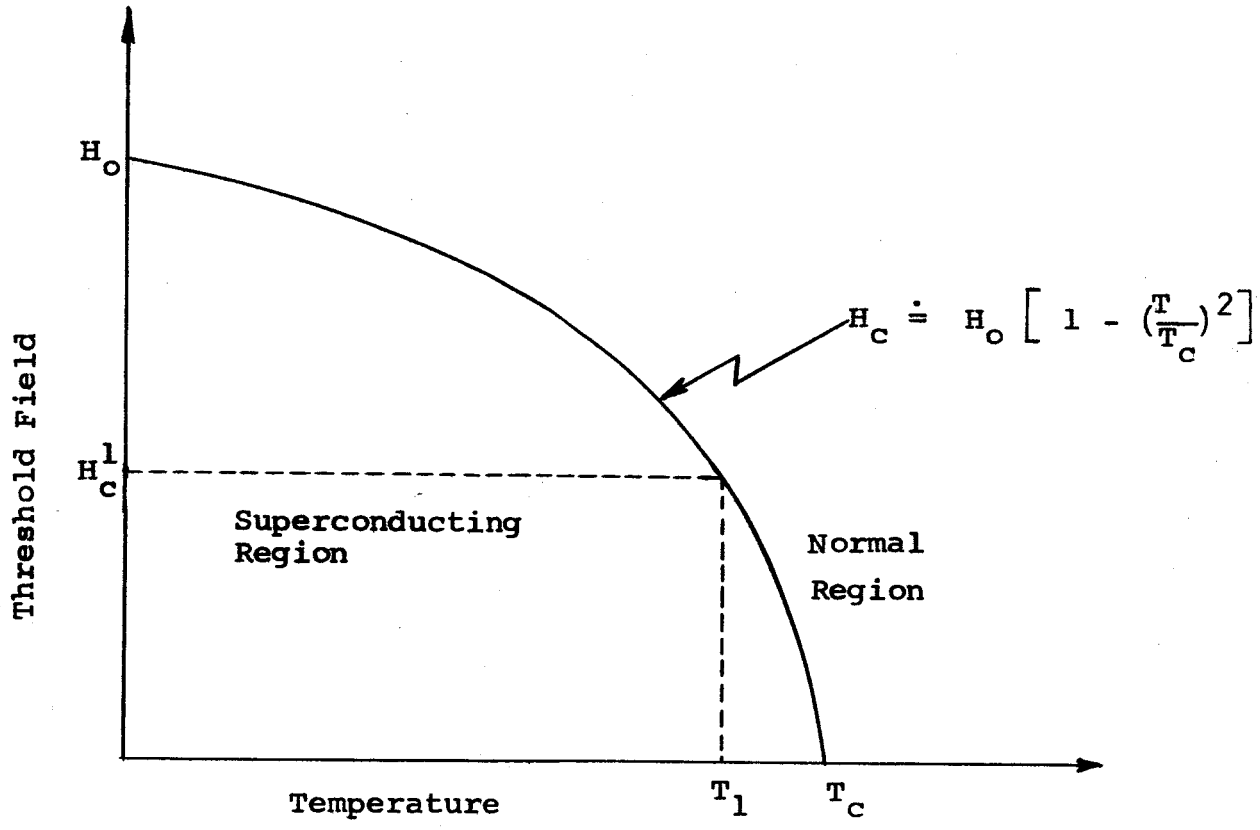

Figure 16

H_c - T Curve

Unfortunately, the present understanding of superconducting and normal metals is still far from this goal. In fact, there is still an inability to calculate the actual critical temperature of any superconductor. However, there have been several qualitative theories proposed which to some degree describe the properties of at least an ideal superconductor. One must realize the difficulty of the problem, which lies in the extreme smallness of the energy involved. For, at absolute zero, the energy gap between the superconducting and normal phase is on the order of 10^{-8} ev per atom; whereas, for a normal metal the Fermi energy of conduction electrons is on the order of 10 to 20 ev.

One of the most successful theories is the one postulated by Bardeen, Cooper and Schrieffer -- the so-called BCS theory.[11] This theory accounts for all the main facts of superconductivity, which are: (1) a second-order phase transition at the critical temperature; (2) an electron specific heat varying as exp $(-T_o/T)$ near absolute zero; and other evidence of an energy gap for individual particle-like excitations; (3) the Meissner effect of zero magnetic induction in the superconducting state; (4) effects related to infinite conductivity; and (5) the dependence of the critical temperature on isotropic mass.

The BCS theory considers that the basic interaction accounting for superconductivity lies with a pair (as opposed to single electron-phonon interaction) of electrons through an interchange of virtual phonons, those with very short lifetimes. This can be intuitively understood by consideration of the following.

The distortion of a lattice by a moving electron gives rise

to a phonon. Further, the distortion of the charge distribution of the lattice results in a propagating fluctuation which in turn affects a second electron some distance away when the wave reaches its location. The conclusion then is that superconductivity occurs when the attractive interaction between two electrons by means of phonon exchange overrules the usual repulsive screened coulomb interaction. In addition, the BCS theory formulizes the normal state by the Block model,[12] which deals with the effect of the periodic field of the lattice on a single electron.

A number of possible explanations have been offered to indicate what fundamental effects might limit the speed of transition between the normal and superconducting state. Most of these predict switching times far shorter than what is observed. One suggestion of interest, proposed by Nethercot,[13] predicts a longer time and is derived relatively directly from the BCS theory.

Briefly, Nethercot states that the present explanation is based on the switching speed being limited by a spatial rather than purely time limited (temporal) effects: that is, at fast switching speeds (high frequency) the skin depth becomes so small that this thin layer cannot change its state due to the large adjacent volume of unswitched material. Therefore, it doesn't seem reasonable that these skin depths could change state in times on the order of 10^{-10} seconds since it can be expected that the properties of the film would be considerably altered by the adjacent material.

3.2 Superconductor Switch Capability Analysis

3.2.1 The Switching Scheme

The switching scheme planned was to vary the magnetic field at the surface of a superconductor either by external fields or internally developed fields such that the superconductor is alternately switched from the superconducting state (zero d.c. resistance) to the normal state (finite resistance). It was planned to use the following techniques to accomplish the above:

1. Place a modulating field coil coaxially with the main field source, as shown in Figure 7, such that the field of the coil would alternately add positively and negatively to the main source field sufficiently to produce a net field alternately less than and greater than the critical field of the sample.
2. The sample itself, placed in a d.c. magnetic field of magnitude just less than the critical field, would be wrapped in a field coil to which an alternating current is applied. The two fields would combine to produce a switching field.
3. Instead of an external d.c. source field, the sample would be allowed to carry a current sufficient to produce at its surface a magnetic field just less than the critical field. Then either a modulating coil, as in item 1 above, or a field winding, as in item 2 above, would be used to complete the switching action.

Unfortunately, the aforementioned difficulties with the liquid helium dewar thwarted all attempts to obtain specific data from experiments conducted following the above procedures.

One of the abbreviated experiments using the external modulation method and a coil of superconducting wire showed some evidence of a switching time that followed 60 cycles; however, no definite conclusions could be arrived at because of the brevity of the run.

3.2.2 Thin Film Switch Feasibility

Below is a brief discussion of superconducting thin film devices, described in the literature, which indicates the high transition time one might expect if a thin film superconductor were to be used as a controlled rectifier.

Feucht and Woodford[14] have calculated transition times of thin films of tin by using a superconducting radio-frequency mixer. This device uses a thin film of high-purity tin evaporated on a glass substrate which is sandwiched between two pieces of polystyrene having a loop contact of lead embedded in each. Around the unit is wrapped a switching coil to which a radio-frequency local oscillator signal is applied. With this configuration it was determined that the time required to switch the film in and out of the superconducting state was as short as 0.625×10^{-9} seconds.

Young[15] has described a so-called "crossed-film cryotron" which uses a thin-film gate, crossed by a lead control film. This device is interesting since it offers a larger resistance in the normal state than does the wire cryotron, thus offering lower transition times.

From the foregoing it would seem one could be quite optimistic about the superconducting controlled rectifier converter for application where the frequencies are reasonable.

3.2.3 Wire Coil Form Switch Feasibility

Buck[16] describes a superconducting wire device called a "cryotron" which was conceived as a computer component. It consists of a control winding of 0.003 inch niobium wire wound around a 0.009 inch tantalum wire. The niobium winding serves as the control gate which switches the tantalum wire in and out of the superconducting state. In this manner a small current is made to control a large current. The transition time of the cryotron is primarily regulated by the L/R time constant of the device to a limit determined fundamentally by relaxation losses. An estimate of this limit is between 100 and 1,000 megacycles. However, the L/R time constant for these small devices places the transition time in the 10^{-3} second range.

3.3 Conclusion

It is believed that the thin film superconductor has promise as a controlled rectifier because the normal resistance of this configuration can be increased by decreasing the film thickness, which in turn would tend to decrease the transition time. Also, inductance problems are within reason with thin-films.

Preliminary calculations[17] indicate that the amount of wire needed to obtain a reasonable circuit switching factor would result in inductance problems that may exclude superconductor wire forms as controlled rectifiers.

Chapter IV

CONVERTER CIRCUIT ANALYSIS

4.1 Selection of the Best Circuit

Three switch-type circuits were considered from which one was chosen for further study as an LV-HC converter. These circuits are shown in Figures 17 - 19.

The circuit of Figure 17 was discarded because its maximum theoretical efficiency is only 50%; and, since d.c. current flows in the primary winding, a severe demand on transformer design is evident. A similar transformer restriction also tended to rule out the circuit of Figure 18.

The circuit of Figure 10, a bridge-type converter, has many desirable features in that: 1) the maximum theoretical efficiency is 100%; 2) no d.c. current flows in the primary of the transformer, allowing for nominal design of the transformer. Analysis of this circuit was extensively developed[17] and is condensed below into the important points.

4.2 Analysis of the Bridge Type Circuit. A Summary.

For square wave switching stimulation, one possible electrical state of the bridge is shown in Figure 20. Here the "off" resistance of each controlled rectifier is R, while it has an "on" resistance, KR.

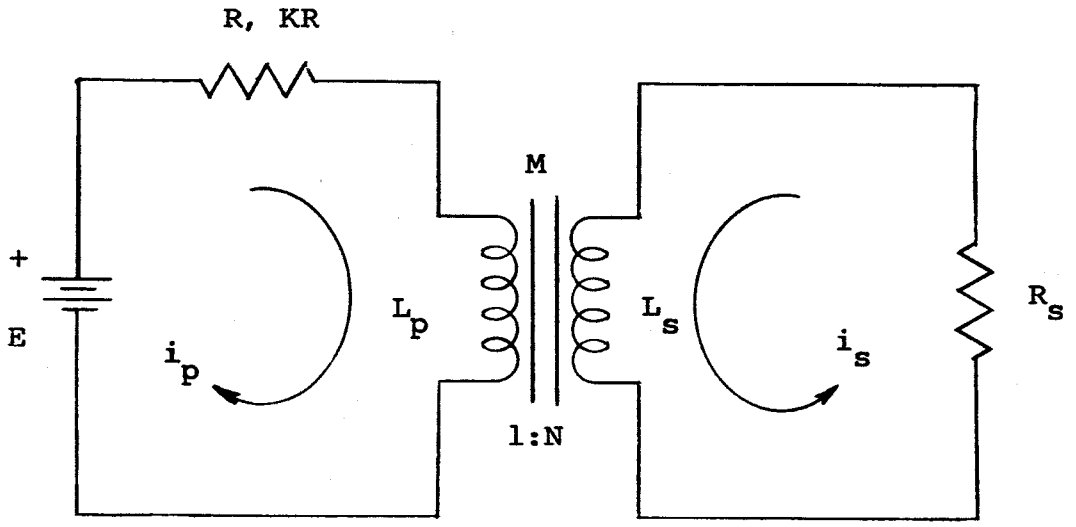

E = open-circuit source voltage

R = total off-field resistance of primary loop

KR = total on-field resistance of primary loop

R_s = total resistance of secondary loop

Figure 17

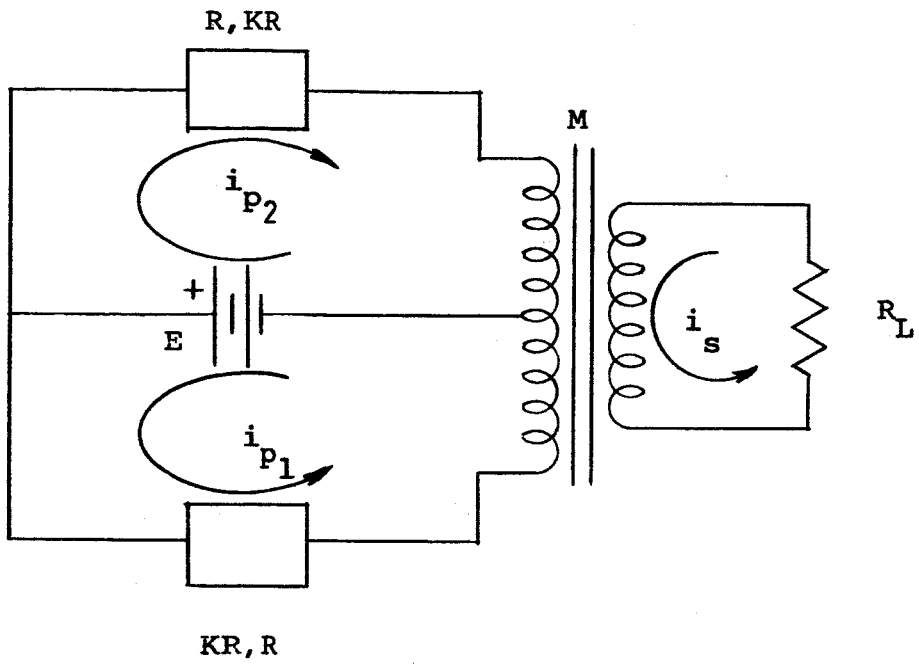

Figure 18

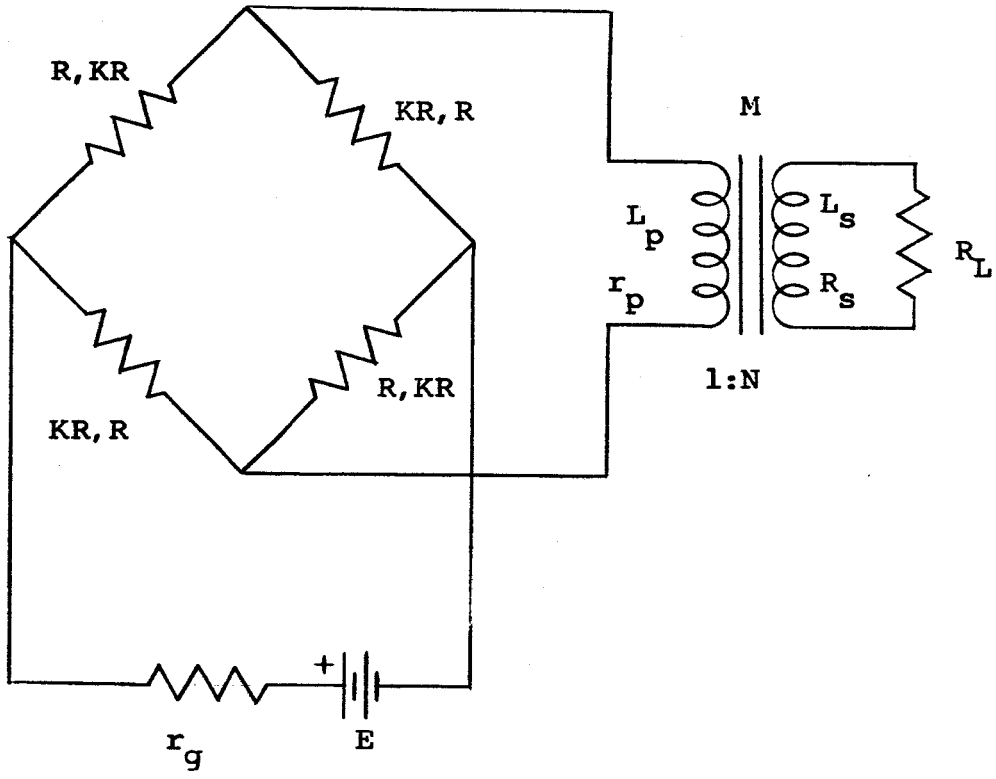

Figure 19

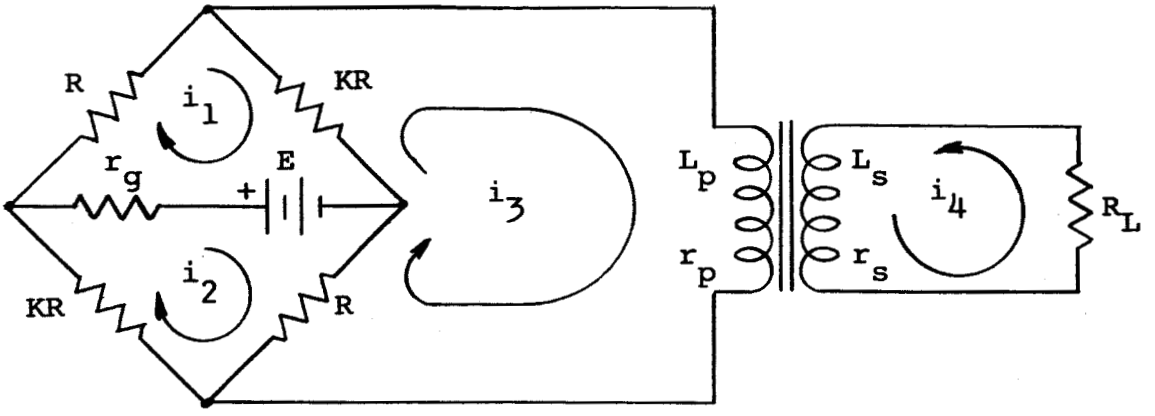

Figure 20

Assemblage and rearrangement of the mesh equations for the bridge circuit in its two states allows one to reduce the problem down to analysis of the equivalent circuit shown in Figure 21(a), which is stimulated by the waveform shown in Figure 21(b).

From the solutions for i_3 and i_4 in the pair of simultaneous differential equations that can be written for the final equivalent circuit, the input power from the source and the power delivered to the load can be calculated. These solutions and calculations have been accomplished to the

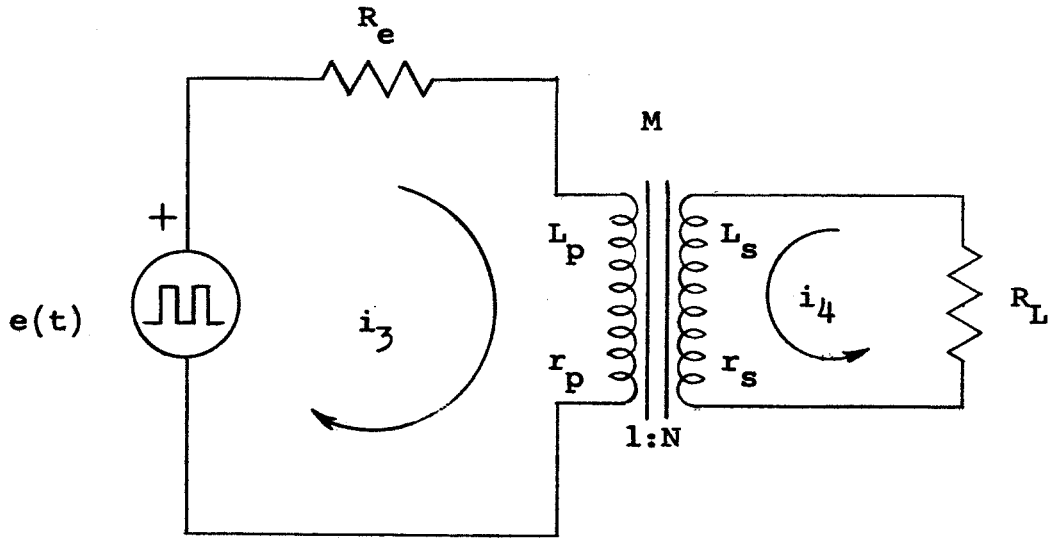

where:

$$R_e = R \frac{2KR + r_g(K+1)}{R(K+1) + 2r_g}$$

and

$$V_e = E \frac{R(K-1)}{R(K+1) + 2r_g}$$

Figure 21(a)

Final equivalent circuit for total operation.

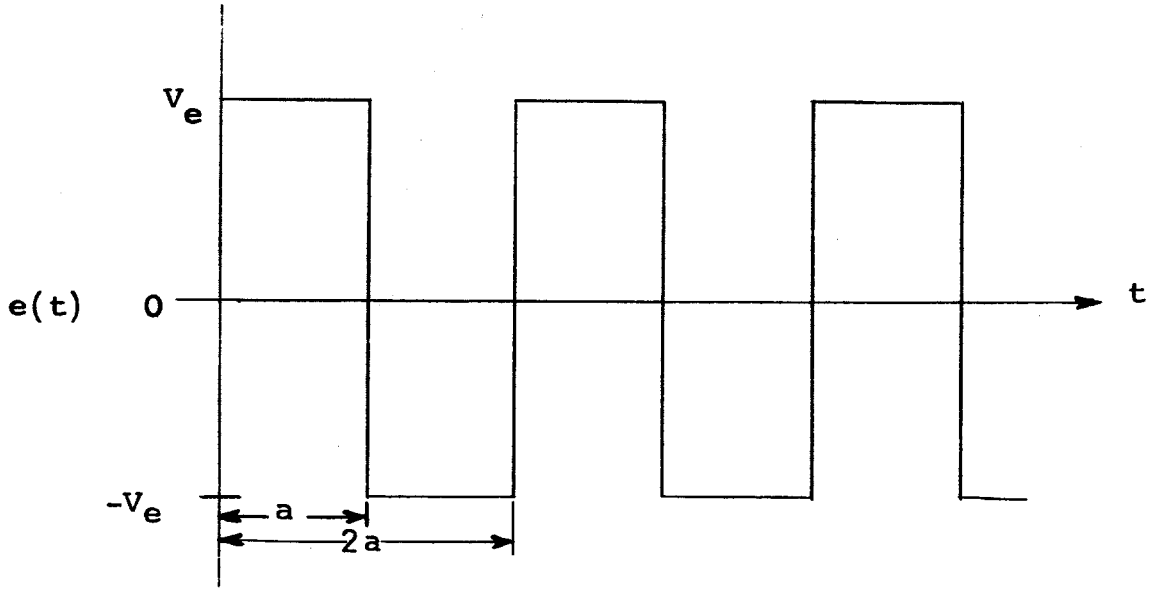

Figure 21(b)
Input waveform for final equivalent circuit.

extent that all currents, voltages and efficiencies can be calculated to any desired degree of accuracy. The expressions are well adapted to digital computer solution.

4.2.1 Analog Computer Solution

Combining the distinct sets of equations that can be written for the original circuit in its two states, allowed a solution by analog computer. A very efficient computer flow diagram for this job was developed and is shown in Figure 22.

The analog computer offers a fast, accurate method of studying the effects of the waveshape of the magnetic field excitation upon the circuit performance. Preliminary computations indicate that the waveshape applied to the MR devices has a substantial effect upon the efficiencies and currents of the MR converter.

If one considers that the controlled rectifiers are magnetoresistors and takes K as 53.4, 145, and 1000 for an InSb disk at room temperature, a Bi disk at 80°K, and a Bi disk at 4.2°K, respectively, the conversion efficiency obtained by computer is 50%, 76%, and 87%, respectively. These are theoretical expectations which do not involve electrical or magnetic losses, of course. It should be remembered, however, that the converter is independent of source voltage; therefore, the efficiencies stated here hold for any input voltage level.

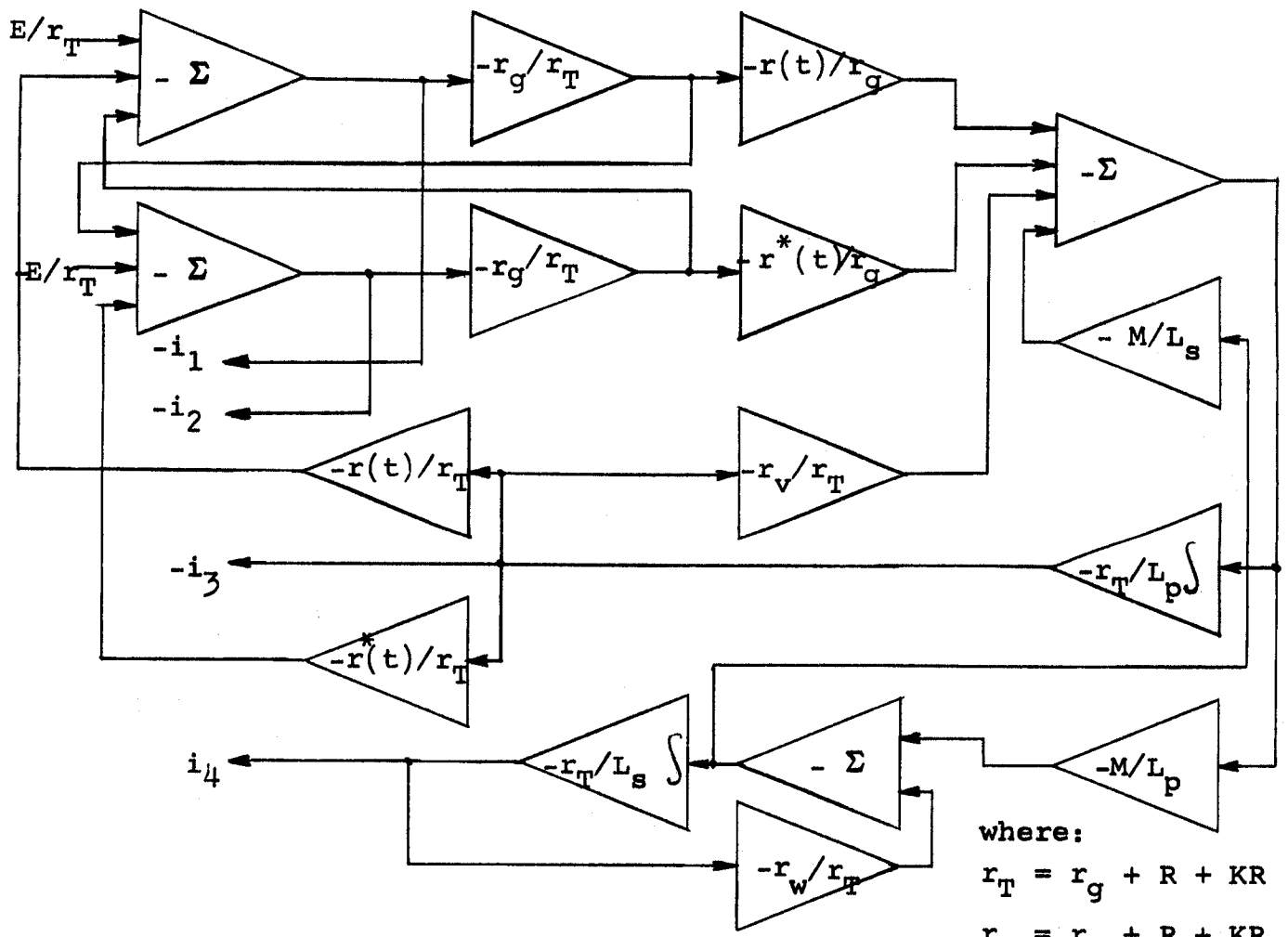

Figure 22

Computer block diagram of the bridge converter
($r(t)$ and $r^*(t)$ are the "off" and "on" magnetoresistor resistance waveforms, respectively)

4.3 Conclusion

The bridge configuration appears to be the best circuit to meet requirements of an LV-HC converter if one uses controlled rectifiers. However, a necessity that still exists is a high magnitude square-wave magnetic field source. A possible solution for this problem will be discussed in Chapter VI.

A conventional magnetic circuit has been analyzed[17] and would be satisfactory for limited applications, but would not be practical for converter applications because of severe power loss, and because of weight and size restrictions.

Chapter V

THIN FIELD EFFECT DEVICE FEASIBILITY STUDY FOR LV-HC CONVERTER APPLICATION

5.1 Technological Review

A derivative of recent advances in thin film technology and theory is the so-called MOS (metal-oxide-semiconductor) insulated gate transistor (sometimes also called a TFT -- a thin-film-transistor).

The MOS transistor is a majority-carrier device in which the current in a conducting channel is modulated by a gate voltage in a typical field-effect manner. Successful MOS devices have been constructed in the surface of a single crystal of silicon,[18] by using thin-films of cadmium selenide,[19] and by using thin-films of cadmium sulfide.[20] A typical plan-view of an MOS device is shown in Figure 23 and is characteristic regardless of the material used. The Cds and CdSe devices are both n-type but the silicon devices can be n-type or p-type by the respective choice of doped silicon. It is understood that p-type devices have also been constructed, using tellurium, at Melpar and RCA.

There are also several variations of the standard MOS transistor, which are also field-effect devices. One of these is called the coplanar-electrode insulated-gate thin-film transistor.[21] The electrode arrangement that characterizes the coplanar device (Figure 24, showing a comparison of this and two more-common units) is said to better facilitate fabrication and to result in on-to-off current ratios on the order of 10^7. Higher spacing precision is obtained by depositing all electrodes on the semiconductor - which results in all electrodes being on the

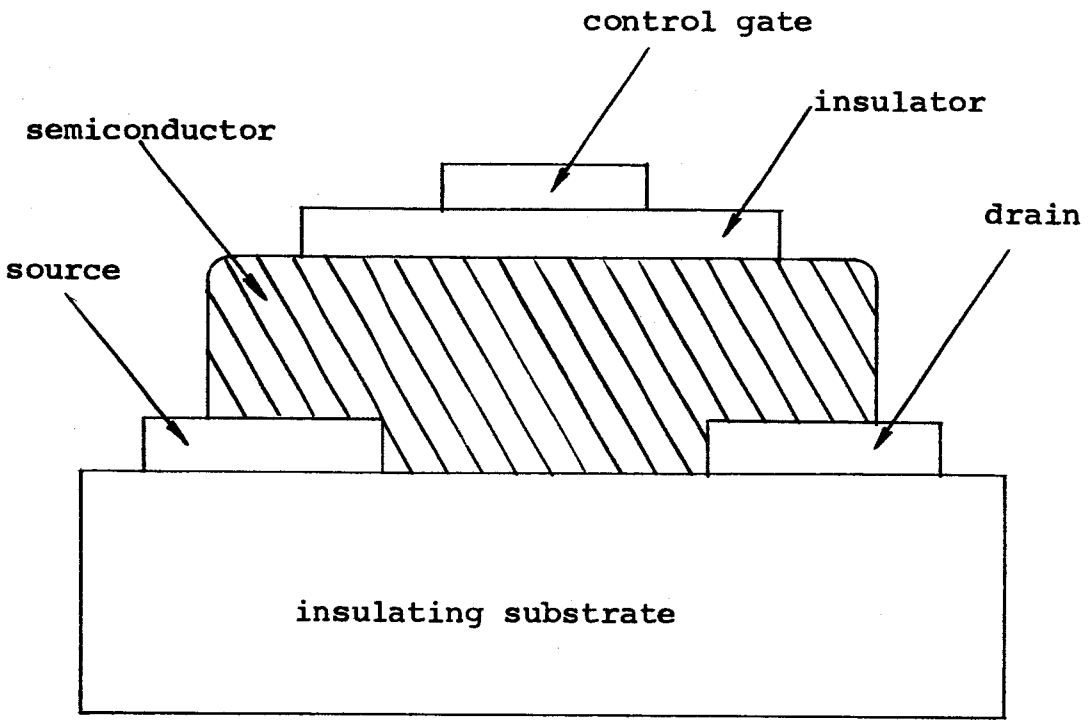

Figure 23

Cross-Section of a type of Thin-Film Transistor

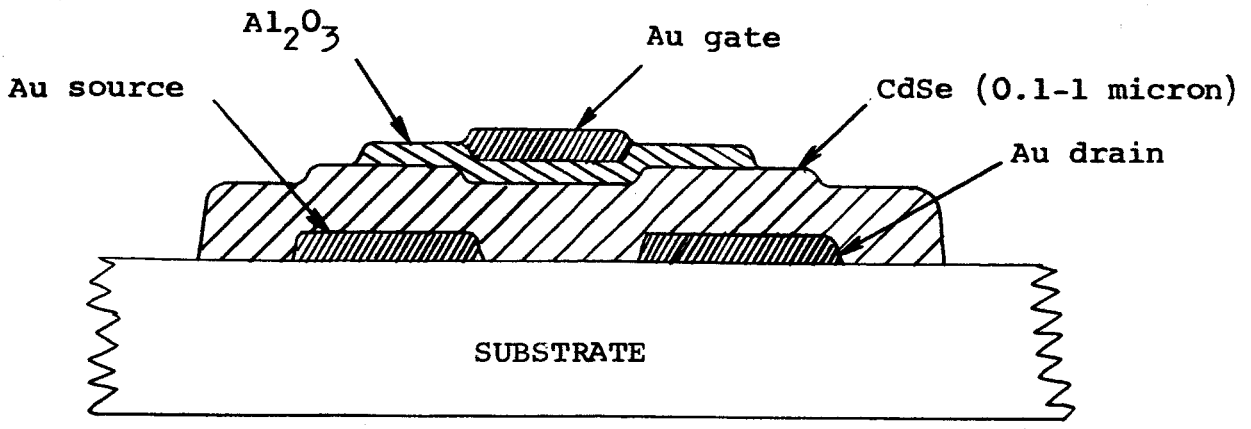

(a)

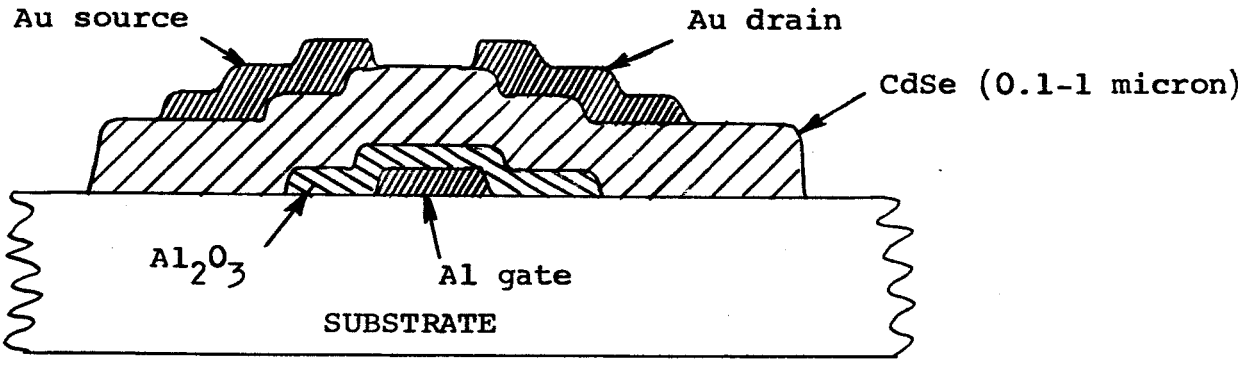

(b)

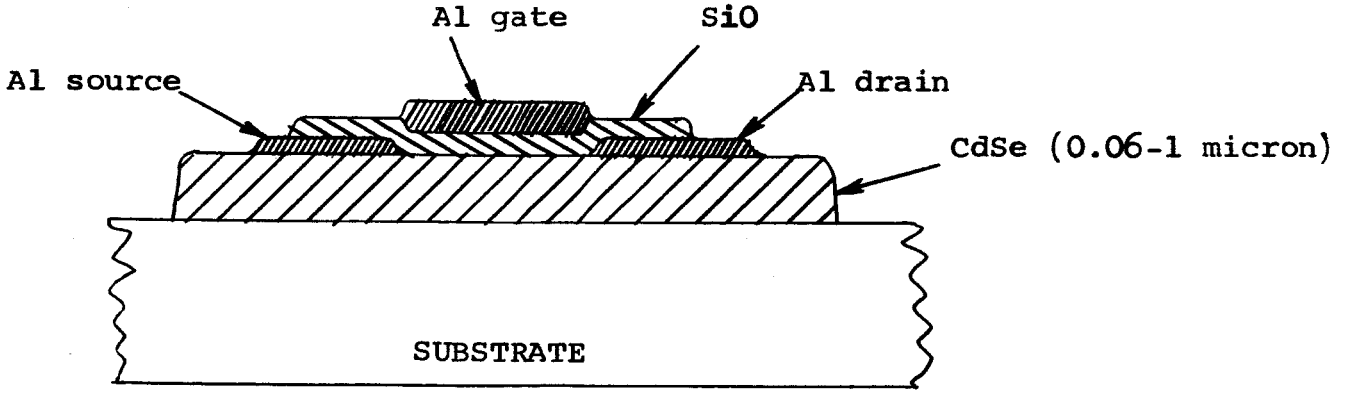

(c)

Figure 24

(a) Staggered-Layer MOS Device

(b) Inverted-Staggered MOS Device

(c) Coplanar MOS Device

same side of the semiconductor. This is in contrast to the other variations which incorporate an interspersion of electrodes.

The gate voltage required for either the onset or pinch-off of drain current is typically around -3 volts. One must realize, however, that these devices, as presently formed, have an extremely high input impedance. If the impedance is to be decreased by increasing the film thickness, this action would necessarily increase the pinch-off voltage.

5.2 Conclusion

Unfortunately, one of the inherent characteristics of the thin-film transistor is a high input impedance that does not show much promise of being lowered. Paralleling a great many of these devices to lower this impedance to an acceptable level -- about one milliohm -- would not be practical. It is not believed that a suitable compromise could be reached between a tolerable pinch-off voltage, response time, and impedance. Therefore, this device would have to be excluded for any practical LV-HC converter.

Chapter VI

THE APPLICATION OF HALL EFFECT DEVICES TO THE LV-HC CONVERTER

6.1 Basic Hall Theory

An expression containing the Hall electric field in an n-type material can be gained immediately from a solution of equation (6) for $\overline{E}$, and is given in the form

$$\overline{E} = \frac{1}{\sigma_n} \overline{J}_n + \frac{\mu_n}{\sigma_n c} (\overline{J}_n \times \overline{H}) \qquad (30)$$

This equation indicates that in a material with a component of magnetic field transverse to the current density, the electric field contains a component which is normal to both $\overline{J}_n$ and $\overline{H}$. This component of electric field is called the Hall field, and the coefficient

$$R_H = - \frac{\mu_n}{\sigma_n c} = - \frac{1}{nec} \qquad (31)$$

is defined as the Hall constant of the n-type material. In general, for materials other than simple metals and degenerate semiconductors, the expression for the Hall constant may be quite a complicated function of energy distributions, scattering potentials and similar properties of the material. This complication results from the fact that in general, the assumption of mean free time being independent of the charge carrier energy (implied in equation 2) is not a valid representation. Thus, for

those materials in which the approximation

$$\frac{d\bar{p}}{dt} = \frac{\bar{p}}{\tau} \tag{32}$$

is not valid, the mean free time between collisions is a function of the electron energy and the dominant scattering mechanism within the crystal.

6.2 The Multi-Terminal Hall Generator[22]

The study to maximize the efficiency of a Hall generator indicated that optimization would occur for a Hall device having an infinite number of output terminals. In the final stages of this study such an N-terminal device, as shown in Figure 25, was analyzed as follows, in abbreviated form.

When the loads are connected across each output terminal, Hall currents will flow through the load and back to the sample in such a direction that a voltage will be induced across the input terminal (in positive direction) by the relation of $V_H = \frac{R_H H I_H}{t}$, where I_H is the Hall current, R_H is the Hall constant, H is the magnetic field, t is the thickness, and V_H is the induced Hall voltage across the input-terminal due to the Hall current I_H. If the resistance of the loads are all the same, all output currents would be the same, as the Hall voltages across each load are the same. Therefore, the total voltage induced across the input terminal by Hall current is the sum of voltages induced by individual output Hall currents.

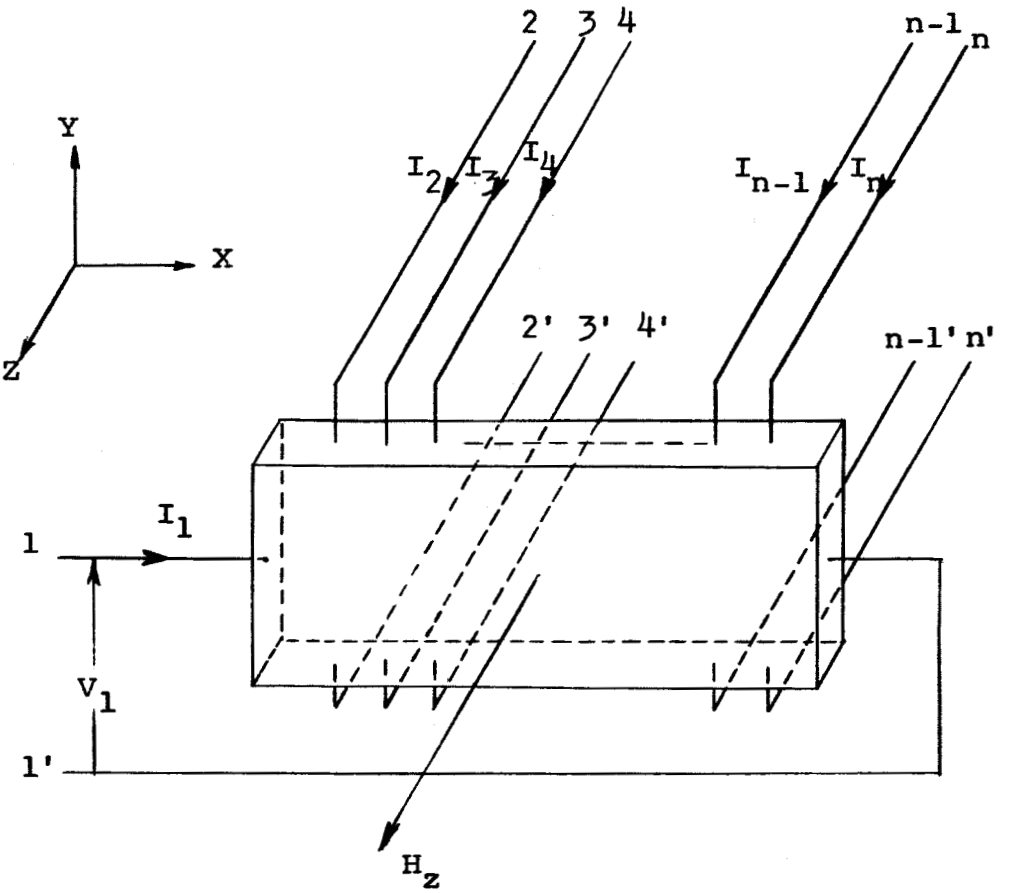

Figure 25

N Output-Terminal Hall Generator

N equations may be derived for an N terminal device which will lead to an equivalent circuit obvious in nature by the form of these equations. The N equations are:

$$V_1 = Z_{11}I_1 + Z_{12}I_2 + Z_{13}I_3 + \text{-----} + Z_{1n}I_n$$

$$V_2 = Z_{21}I_1 + Z_{22}I_2 + Z_{23}I_3 + \text{-----} + Z_{2n}I_n \qquad (33)$$

$$V_n = Z_{n1}I_1 + Z_{n2}I_2 + Z_{n3}I_3 + \text{-----} + Z_{nn}I_n$$

By proper manipulation of these equations most of the desired parameters, such as power delivered to the individual loads, power input, and efficiency can be expressed. One needs then to examine what is necessary to obtain optimum operating conditions from these expressions.

The optimum values of parameters in the efficiency equation were determined analytically and some of them were verified by experiment. These optimum conditions for maximum efficiency are:

1) High mobility
2) Low impurity concentration
3) High mobility ratio
4) High magnetic field
5) Large number of output terminal pairs

A maximum efficiency of 40% for 19 output terminals was obtained experimentally. This could be increased to about 60% by increasing the number of output-terminals to one hundred.

The multi-terminal Hall generator could possibly be used as a d.c. to a.c. converter by applying an alternating magnetic field. The circuitry of such a converter is shown in Figure 26.

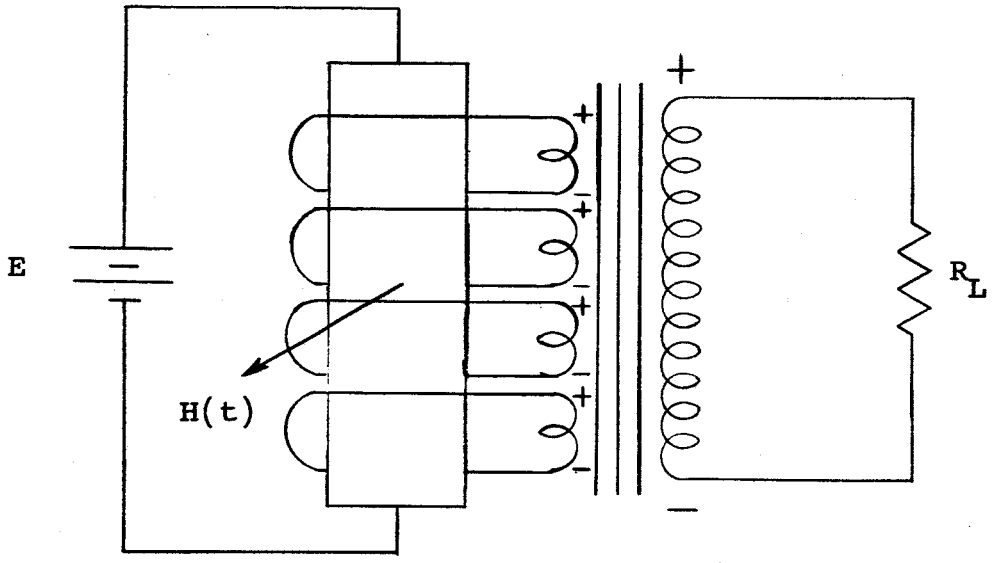

H(t) = Alternating Magnetic Field

Figure 26

Hall Generator as a d.c. to a.c. Converter

For this circuit the output terminals of the Hall generator are connected to the primary coils of a transformer, of which the secondary coil is connected to a load R_L. Each primary coil induces a voltage across the secondary coil so that the total voltage developed across the secondary coil is the sum of voltages developed by each primary coil. The maximum efficiency will be obtained by choosing the load properly such that the impedance looking into each primary coil satisfies the optimum load condition.

6.3 Conclusion

The possibility of using the multi-terminal Hall device should not be ruled out completely for some applications since it may be suitable under more moderate requirements than those imposed by the LV-HC converter. The high current capability and low impedance requirement would be difficult to meet because of contact problems with the Hall terminals: i.e., there is a physical limit to the number of these terminals that can be attached for a particular wire size necessary to carry a desired current load.

Chapter VII

INTRODUCTION TO THE CONCEPT OF OBTAINING A SQUARE WAVE MAGNETIC FIELD USING A SUPERCONDUCTING SHIELD

7.1 Brief Review of the Phenomena of Magnetic Flux Rejection

In 1933 Meisner demonstrated that the magnetic flux is expelled from a superconductor whether it be cooled to the semiconducting state in a constant field, or cooled in zero field and then placed in a magnetic field. Therefore, the magnetic induction (B) of a metal is always zero while in the superconducting state. It follows that if there is no magnetic field inside a superconductor, any current must be superficial. Since the current cannot be strictly superficial, there must be a finite depth to its flow, and therefore a finite depth of penetration of the magnetic field into the superconductor. Following this concept leads to previously derived expressions[23] for this penetration depth. In general one can assume that this depth will be less than 500 Angstroms.

Furthermore, there was shown to be a critical strength for the current flowing in a superconductor in that it must remain less than that required to produce a field equal to the critical magnetic field. This characteristic is the factor that now limits the maximum field of superconducting magnets. With each new breakthrough in material research[24] this maximum is increased proportionally, and these advances appear to be fairly steady.

7.2 Application of the Meissner Effect to Magnetic Field Switching

The complexity of obtaining a high amplitude, square wave magnetic field by conventional means, for a convertor circuit requiring such a field, can be appreciated when one considers what is involved in obtaining a comparatively simple 60 cps sinusoidally varying magnetic field with a peak of just 10 kilogauss. In the design calculation for a magnet of this type a gap of 1-1/4 inches and a pole tip diameter of 1-1/2 inches were considered. Calculations indicated that the core of this magnet would weigh close to 125 pounds, while the entire system would occupy a space of about 2 cubic feet. Since the magnet would draw excessive current from a single-phase line (although the magnet would be highly reactive and not consume much power), power factor correcting capacitors would have to be used. Approximately 60 KVAR of capacity would be required. With this power factor correction the magnet would represent about a 2 kilowatt load, considering conductor and core losses. If one desires to increase the frequency to say 400 cps, this would increase the load from 60 KVA to 400 KVA and, of course, require that thinner laminations be used in the core to hold the iron losses down. One can see then that obtaining a square-wave magnetic field of 25 kilogauss (or even 10 KG) peak by purely conventional means represents a formidable task and appreciable size and weight.

A better solution to the problem may be the use of a controlled, superconducting magnetic shield in an arrangement such as shown schematically in Figure 27.

The principle here, is to vary the magnetic field in which the superconducting shield is placed such that the field at the surface of the shield alternately passes through its critical magnetic field.

7.3 Experimental Evidence of Magnetic Shielding

One successful experimental run was completed using a 10 mil thick niobium sheath to shield a Corbino disk magnetoresistor. For this run the magnetic field was varied through a range of 0-9,500 gauss. The niobium shield material was somewhat impure; nevertheless switching occurred at about the expected magnetic field level.

A typical result of this experiment is shown in Figure 28. One may notice that definite evidence of switching is clear.

7.4 Conclusion

Based on the experimental evidence of the shielding capability that was demonstrated, limited though the evidence was, it is believed that the switchable, superconducting shield technique may be the answer to the problem of obtaining a high amplitude, square wave magnetic field. Though transition time studies were not able to be made, evidence from the literature indicates times in the nanosecond region for small, thin-film devices such as the Feucht and Woodford radio frequency mixer.

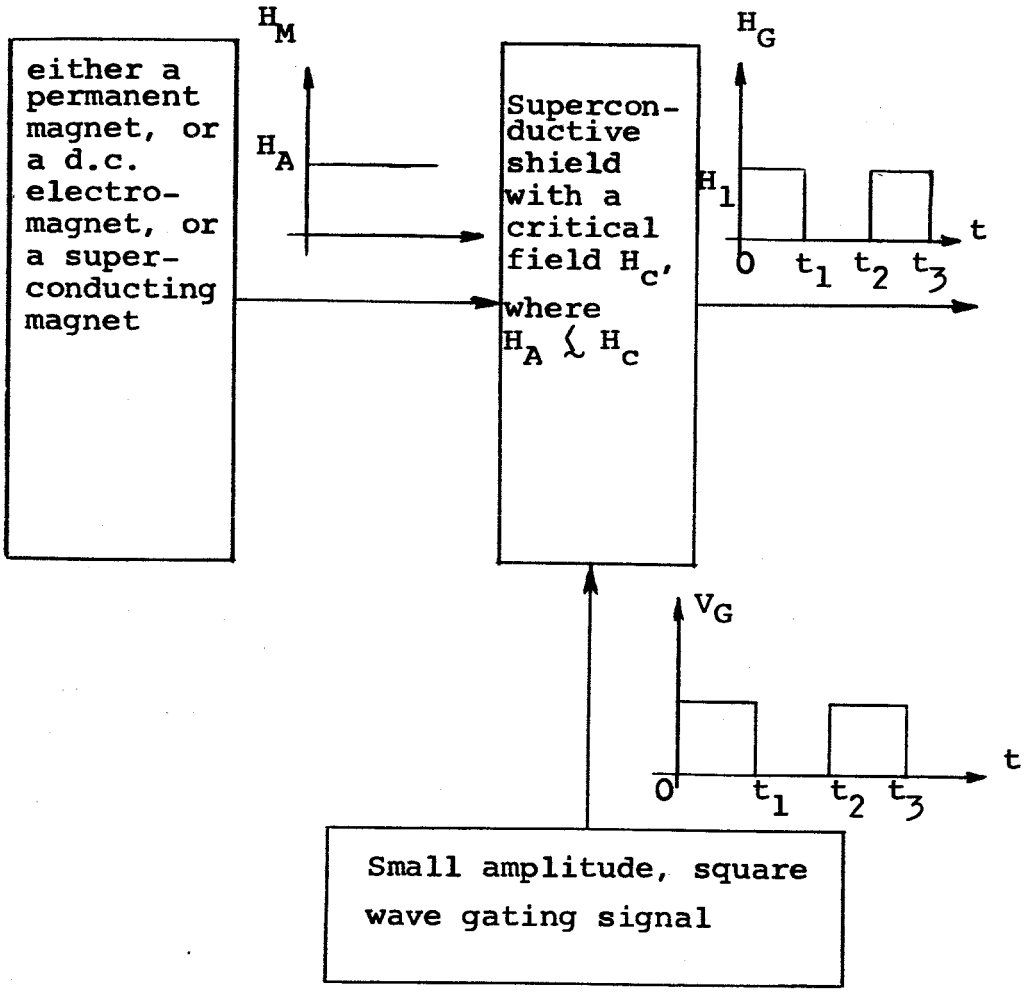

Figure 27

Block Diagram of the Magnetic Circuitry to Obtain a Square-Wave Magnetic Field

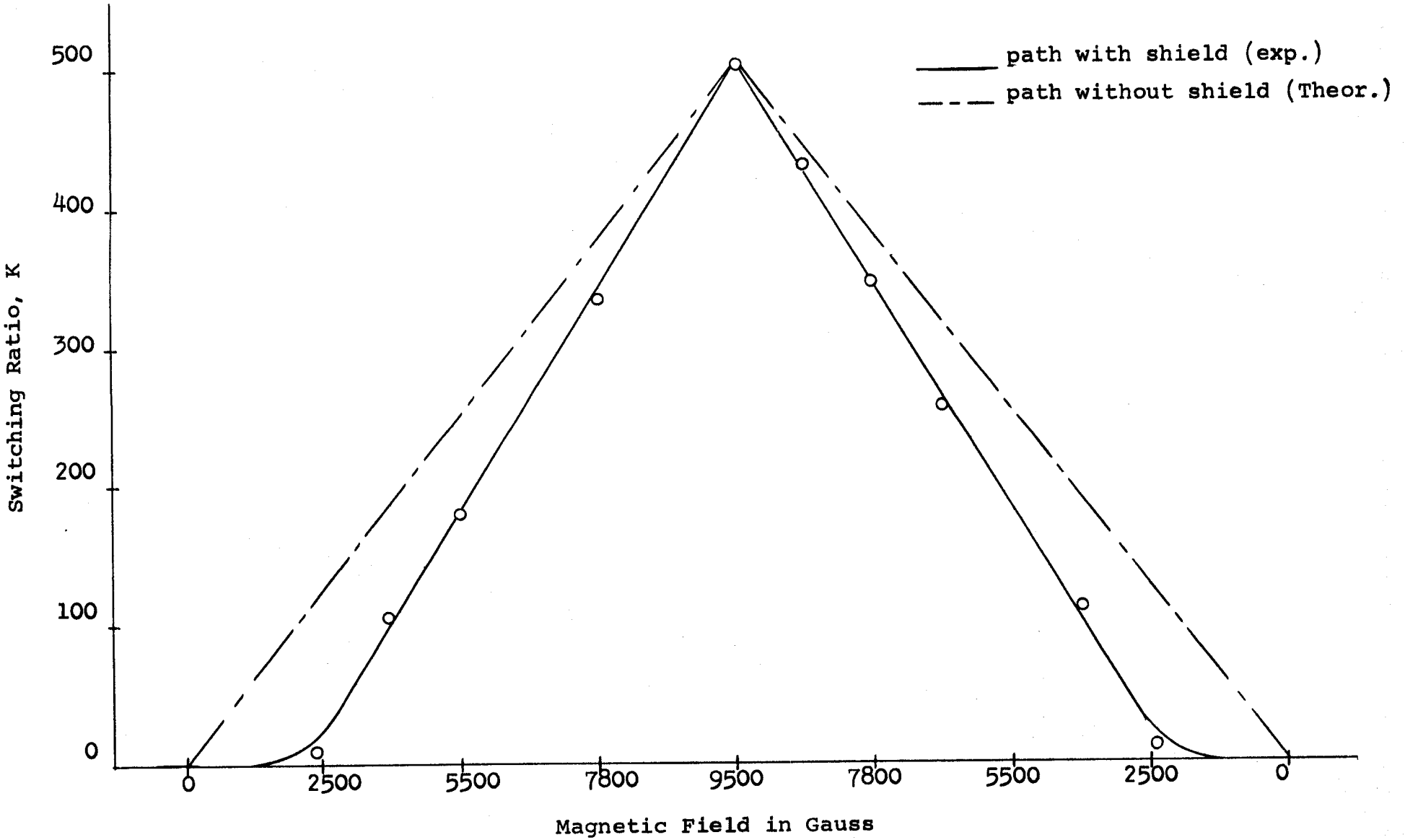

Figure 28

Corbino Disk Sample 9LG with 10 Mil Niobium Shield
Sample Current 300 ma
Temperature 4.2°K

Chapter VIII

CONCLUDING REMARKS

The future prospects for a controlled rectifier LV-DC converter of the types that showed promise in this project are encouraging. It is obvious that the system best suited to the LV-DC converter requirements, and possessing the highest efficiency, would be a bridge circuit employing bismuth Corbino disk controlled rectifiers driven by square-wave magnetic fields from magnetic sources using switchable superconducting shields. Such a system could be completely contained in the cryogenic environment if desired. This system is also of interest because a present day superconducting material (Nb_3Sn) has a critical temperature nearly that of liquid hydrogen, which is a present on-board space craft consumable. Also, there are presently a few simple and compact mechanical cryogenic refrigerators that have a temperature capability near $20^{\circ}K$.

REFERENCES

1. "Low Input Converter Study," Progress Report, Electro-Optical Systems, Inc., August 1962.

2. Shockley, William, Electrons and Holes in Semiconductors, D. Van Nostrand Company, Inc., New York, 1950, 180.

3. Ziman, J.M., Electrons and Phonons, Oxford Press, London, 1960, 491.

4. Adams and Holstein, "Quantum Theory of Transverse Galvano-magnetic Phenomena," J. Phys. Chem. Solids, Vol. 10, 1959, 254-276.

5. Sladek, R.J., "Magnetoresistance of High Purity InSb in the Quantum Limit," J. Phys. Chem. Solids, Vol. 16, 1960, 1-9.

6. Bate, R.T., R.K. Willardson, and A.C. Beer, "Transverse Magnetoresistance and Hall Effect in N-Type InSb," J. Phys. Chem. Solids, Vol. 9, 1959, 119-128.

7. Green, Milton, "Corbino Disk Magnetoresistivity Measurements on InSb," Journal of Applied Physics, Vol. 32, No. 7, 1961.

8. Corbino, O.M., Atti. Acad. Nazl., Lincei 20, 1911.

9. Kleinman, D.A. and A.L. Schawlow, "Corbino Disk," Journal of Applied Physics, Vol. 31,(1960),2176.

10. Matthias, B.T., Progress in Low Temperature Physics, Vol. II, Interscience, 1957.

11. Bardeen, J, L.N. Cooper and J.R. Schrieffer, "Theory of Superconductivity," Physics Review, Vol. 108,(1957),1175.

12. Brillouin, Wave Propagation in Periodic Structures, Dover: 1953.

13. Nethercot, A.H., Jr., "Superconducting-Normal Transition Time," Physical Review Letters, Vol. 7,(1961),226.

14. Feucht, D.L., and J.B. Woodford, Jr., "Superconductor Transition Time Measurements Using a Superconductive Radio Frequency Mixer," Journal of Applied Physics, Vol. 32, (1961), 1882.

15. Young, D.R., "Recent Developments in High Speed Superconducting Devices," Brit. J. Appl. Phys., Vol. 12, (1961), 359.

16. Buck, D.A., Proceedings of the IRE, Vol. 44, (1956), 482.

17. Harper, B.J., R. Bechtel, and W.W. Grannemann, "A Study of the Hall Effect and Magnetoresistance for Low Voltage, High Current, DC to AC Conversion," University of New Mexico Technical Report EE-96, (July 1963), 45 - 48. (Note the misprint on page 47. The critical field of niobium at 4.2°K is 1500 gauss, not 6000 gauss.)

18. Herman, F.P., and S.R. Hofstein, "The Insulated-Gate Field-Effect Transistor," presented at the Electron Devices Meeting, Washington, D.C., October, 1962, (Attended by the Authors). Published, Proc. IEEE, Vol. 51, (1963), 1190.

19. Shallcross, F.V., "Cadmium Selenide Thin-Film Transistors," Proc. IEEE, Vol. 51, (1963), 851; and Shallcross, F.V., "Evaluation of Cadmium Selenide Films for Use in Thin-Film Transistors," RCA Review, Vol. 24, (1963), 676.

20. Weimer, P.K., "The TFT - A New Thin-Film Transistor," Proc. IEEE, Vol. 50, (1962), 1462; Borhan, H., and P.K. Weimer, "An Analysis of the Characteristics of Insulated-Gate Thin-Film Transistors," RCA Review, Vol. 24, (1963), 153.

21. Weimer, P.K., F.V. Shallcross, and H. Barkan, "Coplanar-Electrode Insulated-Gate Thin-Film Transistors," RCA Review, Vo.. 24, (1963), 661.

22. For a complete coverage of this topic see Pak, S.S., and W.W. Grannemann, "The Multi-Terminal Hall Generator," University of New Mexico Technical Report EE-106, May 1964.

23. Bechtel, Richard and W.W. Grannemann, "Methods for DC to AC Conversion," UNM Progress Report 62, December 1964.

24. "Synthesis, Characterization, and Application of Superconducting Niobium Stannide (Nb_3Sn)," RCA Review, Special Issue, Vol. 25, No. 3, September, 1964.